Control Chart for Detecting Assignable Cause Variations in Non-normal Production Process

BY

SHEIKH YASIR ARAFAT

Student ID: 20131208016

A Thesis Presented to the

DEPARTMENT OF STATISTICS

BANGABANDHU SHEIKH MUJIBUR RAHMAN SCIENCE & TECHNOLOGY UNIVERSITY

GOPALGANJ-8100, BANGLADESH.

In Partial Fulfillment of the

Requirements for the Degree of

MASTER OF SCIENCE

In

STATISTICS

JUNE, 2019.

BANGABANDHU SHEIKH MUJIBUR RAHMAN

SCIENCE & TECHNOLOGY UNIVERSITY

GOPALGANJ-8100, BANGLADESH.

DEPARTMENT OF STATISTICS

This thesis, for course STA508, written by **SHEIKH YASIR ARAFAT** (Student ID:20131208016) under the direction of his project supervisor **MD. MURAD HOSSAIN**, has been presented and accepted by the Department of Statistics, in partial fulfillment of the requirements for the degree of **MASTER OF SCIENCE** IN **STATISTICS.**

X

Md. Murad Hossain
Supervisor

X

S.M. Nasim Azad
Chairman, Department of Statistics,BSMRSTU.

To my respected parents and teachers

ACKNOWLEDGMENTS

Firstly, I am so much thankful to the Almighty Allah for His supports in every instant of my life and proving me the opportunity to complete this thesis. Secondly, I would like to thank my parents for their numerous prayers and struggled that assist me to reach here.

Although I submitted this thesis due to the requirement of my own M.Sc. in Statistics degree, but it is neither my alone journey nor effort. Therefore, I would like to express my gratitude to few eminent person who supported me a lot to pursue my objective.

First of all, I would like to evolve my profound and pious thankfulness to Md. Murad Hossain, my M.Sc. thesis supervisor for his topnotch technical support that generates a classy environment of research as well as his care to my personal lives and prosperity. I owe an immense amount of appraisal for his incisive supervision, precious guidance and indefeasible help at each and every steps of this thesis, without which it would be impossible for me to hold this thesis at daylight. He leads me like his junior brother which unties the chance to share my problems with him hermitically.

A special gratitude I give to my B.Sc. project supervisor Md. Pear Hossain, whose contribution in worthy suggestions and encouragement, helps me to commensurate my thesis. I thank him for his guidance that engenders new ideas and explanation to implement those ideas more effectively. He also suggests and encourages me to work in industrial quality control. I am really grateful to him for providing me such an interesting and realistic idea as my thesis topic. Likewise, I am deeply grateful to S.M. Nasim Azad, the honorable chairman of Department of Statistics for accepting me as a M.Sc. thesis student in his department and for being so much supportive and friendly throughout my thesis period.

I am very thankful to Md. Kamal Hossain, the former honorable chairman of Department of Statistics for inspiring me to study statistics and helping me to take some important decisions of my life. He is the only one person who believes in me from the very beginning of my life as a student of statistics. He encourages me to see big dreams and educates how to fulfill them. Without his stimulating suggestions and encouragement, it won't be possible for me to secure first position in B.Sc. May Allah mercy him with His full blessings and give him the most prestigious haven.

Special thanks to Nishith Kumar, the first honorable chairman of Department of Statistics for giving me not only the opportunity to take admission into his department but also his appropriate suggestion to select my M.Sc. thesis field of research. After that, I would like to

express my thankfulness to all of my honorable teachers of Department of Statistics who teaches me not only everything about statistics but also the ethics of life.

I am really obliged to my friends specially Moh. Mizanur Rahman, M. Sadman Zihan and Prosenjit Mondal for their support and my classmates as well. Finally, I want to laud all those who contributed me the possibility to complete this thesis.

SHEIKH YASIR ARAFAT

TABLE OF CONTENTS

LIST OF FIGURES

LIST OF TABLES

LIST OF ABBREVIATIONS

MLE	Maximum Likelihood Estimation
PDF	Probability Density Function
CDF	Cumulative Distribution Function
CF	Characteristics Function
MGF	Moment Generating Function
UCL	Upper Control Limit
LCL	Lower Control Limit
CL	Central Line
UPL	Upper Probability Limit
LPL	Lower Probability Limit
ARL	Average Run Length
SDRL	Standard Deviation of Run Length
MRL	Median of Run Length
RL	Run Length
SPC	Statistical Process Control
EWMA	Exponentially Weighted Moving Average
CUSUM	Cumulative Sum
PCI	Performance Comparison Index
EQL	Extra Quadratic Loss
RARL	Relative Average Run Length
IMD	Inverse *Maxwell* Distribution
IMEWMA	Inverse *Maxwell* Exponentially Weighted Moving Average
IMCUSUM	Inverse *Maxwell* Cumulative Sum

ABSTRACT

Variations are present in the outcome of every process. Different variations of control charts are implemented to identify and eliminate the assignable cause variations. Shewhart type charts are useful to address transient assignable causes, whereas memory type charts are more sensitive to persistent assignable causes. These charts are developed for normal distribution which is not always exhibit in every real-life scenario. As a candidate of memory type control chart, EWMA chart is usually implemented to detect small variations. Though the production scheme contains both transient and persistent special cause variations, we need control charts that can handle both variations and make the process statistically in-control. In this thesis to accomplish these purposes, we have designed two new control charts, namely IMEWMA and Combined IM-VEWMA control charts, where CIM-VEWMA is designed by combining the feature of V_{IM} and IMEWMA charts. The IMEWMA chart is very sensitive to small variations and CIM-VEWMA can accommodate both small and large shifts of an inverse *Maxwell* process. Several run length properties including ARL, SDRL, MRL, EQL, RARL and PCI are implemented for analyzing the performance of the proposed control charts. Comparisons are made and evince that the proposed charts surpass from some existing charts to control inverse *Maxwell* scheme. The pragmatic application on the lifetime of cars brake pad is provided for explicating the implementation suitability and performing superiority of the developed charts.

CHAPTER ONE
INTRODUCTION

1.1 Background

In this thesis, we introduce three control charts namely IMCUSUM, IMEWMA and CIM-VEWMA control charts. We develop these control charts under inverse *Maxwell* distribution. Several distributional properties of the inverse *Maxwell* distribution including skewness and kurtosis, Fisher information, moment generating function (MGF), characteristics function (CF) and Entropy are discussed. Then performances of the developed charts are assessed by different run lengths properties. Simulated data has been implemented to visualize the simple design procedure. Finally, the application of these charts on real life are given.

Production scheme is the conversion of a group of inputs into desired outputs. The outputs of a process are not same. They contain variations. Walter A. Shewhart, a pioneer of Statistical Process Control (SPC) distinguished two kinds of variation in processes that affect production characteristics: common or random cause vitiation and assignable or special cause variation [1]. The totality of the collection of effects of a complicated interaction of random or common causes usually associates with random variations [2]. The assignable cause variation may also be categorized into two types namely transient, which appear in the process for short-term and persistent, which is sporadic and present until elimination [3]. Due to the lone presence of common cause variations, the scheme is apprehended to be ‘stable’ or ‘statistically in-control’. If the process contains special cause variations that don’t belong to random cause variations, then the scheme is called ‘unstable’ or ‘statistically out-of-control’. We need to find out these assignable cause variations and take adequate actions to make the process ‘in control’.

SPC is implemented to study and manage variations. It is a merger between industry and statistical techniques, introduced and popularized by Shewhart and Deming. In this methodology we have seven tools, often named as the ‘magnificent seven’ or ‘SPC tool-kit’ including histograms, cause and effect diagrams, scatter diagrams, check sheets, defect concentration diagrams, Pareto charts and control charts [4]. All these SPC tools are applied to any scheme to detect and reduce variations. Among all these tools the last one is the most sophisticated tool and frequently used to identify variations and damages for both normal and non-normal process [5] [6] [7].

Control chart is extensively employed to detect the stability of the process parameters and determine the process capabilities in the agricultural sector, health sector and industrial sector [8]. The conventional control charts include the memoryless control charts and memory type charts. Shewhart type control chart is usually considered as memoryless control chart and mostly used to detect transient cause variations which indicate change shifts in location or scale parameters. It is based on the last sample information of any scheme while the memory type charts accumulate total information in the entire series of sample observations to identify persistent cause variations. The popularly applied kinds of memory control charts include exponentially weighted moving average (EWMA) and cumulative sum (CUSUM) control charts designed by Roberts and Page respectively [9] [10]. They are very impressible to small and moderate variations because these charts use both past and present information. To have a balance between the two types of charts and get protection against all kinds of shifts including large and small variations, several scholars advise to combine either EWMA or CUSUM chart with Shewhart chart.

All the above-mentioned individual and combined charts assume normality. For a scheme based on normal distribution the main parameters of the Shewhart chat is lower control limit (LCL), central line (CL) and upper control limit (UCL). The plotting statistic of this chart is the mean of the subgroups. Assume that X_i is distributed as normal scheme with known mean μ_0 and variance σ^2. Now to check the permanence of this scheme based on the classical Shewhart control chart the plotting statistic,$\bar{x}_i$ and the control structures are defined as

$$\bar{x}_i = \frac{\sum_{i=1}^{n} x_i}{n},\ LCL = \mu_0 - L\frac{\sigma_0}{\sqrt{n}},\ CL = \mu_0 \text{ and } UCL = \mu_0 + L\frac{\sigma_0}{\sqrt{n}}\,. \tag{1.1}$$

In (1.1), n represents the sample size and L indicates the control structure coefficient that is estimated based on either false alarm rate or in-control average run length (ARL_0) and these are fixed by the researchers before the analysis. To monitor this normally distributed scheme based on EWMA control chart, the control structure is

$$\begin{gathered} Z_i = \lambda X_i + (1-\lambda)Z_{i-1}, \\ LCL = \mu_0 - L\sqrt{\frac{\lambda}{2-\lambda}(1-(1-\lambda)^{2t})}, \\ CL = \mu_0 \text{ and} \\ UCL = \mu_0 + L\sqrt{\frac{\lambda}{2-\lambda}(1-(1-\lambda)^{2t})}. \end{gathered} \tag{1.2}$$

In (1.2) λ denotes the smoothing constant which value lies between 0 and 1, X_i and Z_{i-1} provide the present and past information respectively.

The CUSUM procedure acts by two approaches where one aggregates the alternations upward from a pre-specified fixed value and another works for the downward alternations. Due to this reason, we denote the 1st case as $c^+$and the later one as c^- where they represent the upper and lower CUSUM statistics respectively. Assume that, X is a process where X_i is its ith sample observation and for this process the pre-specified fixed value is μ_0 then these two plotting statistics can be expressed as

$$\begin{aligned} c_i^+ &= \max[0, X_i - (\mu_0 + k) + c_{i-1}^+] \text{ and} \\ c_i^- &= \min[0, X_i + (\mu_0 - k) + c_{i-1}^-] \end{aligned} \tag{1.3}$$

where, k represents the reference value of CUSUM chart and for normal distribution it is defined as $k = \delta/2$, here δ denotes the amount of variations that a scheme contains. Primarily, we consider c^+ and c^- as zero, when finally we get the values of these estimators then we plot them against either the upper or lower control limits, denoted by h. Based on the pre-specified in-control ARL, we have to estimate h but usually it lies between 4 or 5 times of the standard deviation of the process.

In real-life, we get data from different sectors that don't follow normal distribution including health care, industry, engineering and agricultural sectors. In statistics we have different types of distributions to model data such as *Weibull* distribution, *Gamma* distribution, *Exponential* distribution, *Extreme* value distribution etc. But in real life we got different kinds of situations where these types of popular distributions are not suitable. For this we have to use other statistical distributions to fit the life time data. Tyagi & Bhattacharya [11] [12] used *Maxwell* distribution as a possible life time distribution.

In physics, *Maxwell* distribution was used to develop the velocity distribution of granular gases those are force free [13]. Molecules are ejected when materials are dismissed from a solid surface by expounding laser beam in it and this process is called laser ablation. The speed of these molecules are be modeled by *Maxwell* distribution [14]. This distribution is also frequently used in chemistry [15]. In the literature we observe that the velocity in which the airbag gases reacts follow *Maxwell* distribution [14] [16].

Now, in statistics, an inverse distribution is a probability distribution of the reciprocal or inverse of a random variable. This type of distribution is used not only in mathematical

statistics but also in various fields such as engineering, agricultural and industrial sector to describe different phenomena and to make quantitative analysis [17]. For example, in the study of a renewal process for human population, it is applied to describe the net maternity function in demography [18]. In the literature, we see that the maternity function for successive generations is expressed as the inverse distribution except for first generations. [19]. In aerial surveys of agricultural land, field sizes are measured in length and width and in general these data are tending to be positively skewed. The inverse distributions are used for modelling crop field size [20]. In industry the length of employee service is also determined by the inverse distribution. In the literature, we also see that inverse distribution is used as a candidate distribution for risk analysis [21].

Because of the vast applicability of both *Maxwell* and inverse distributions, Arafat et al. derived and popularized the inverse *Maxwell* distribution from *Maxwell* distribution [22]. Inverse *Maxwell* distribution also appears in [23], [24], [25]. In [23] they constructed the PDF of inverse *Maxwell* distribution along with its' few statistical properties. They also derived survival and hazard function to imply this distribution in life-time modeling. In [25], under the assumption of Size- Baised sampling, the Bayesian estimate of the scale parameter has been obtained. The bayes estimator is also estimated thorough the squared error of loss function and the risk functions are also derived. In 2014 Lata and Srivastava discussed the estimation problem of size-biased inverse *Maxwell* distribution in [24]. In that paper they estimated the parameter by MLE and method equation estimation. Several properties of this distribution are obtained along with its survival and hazard curve.

In industrial sector production processes are frequently monitoring to run the industry most effectively as possible and to retain the products quality as granted. Though the quality of a service or product is the most significant criteria for choosing that service or product and variation elimination is one of the most popular approach to improve the quality of a scheme. Hence, it derived us to detect variations quickly and eliminate them so that we can get a more standard scheme.

To monitor a *Maxwell* production process Hossain et.al. proposed a Shewhart type control chart named *V* control chart [26]. They also constructed MCQ and MMCQ control chart for mixture *Maxwell* parameters [27]. These control charts are frequently applied in noon-normal production process. Arafat et al. proposed V_{IM} control chart under the assumption of inverse *Maxwell* distribution and it is a Shewhart type control chart that can detect large

variations [22]. The performance is evaluated and proposed chart is constructed for both for the probability limits and L- sigma limits using various performance measures like power curves and run length properties. Finally, they have implemented the newly proposed chart under both simulated and real-life data sets.

1.2 Outlines of the remaining chapters

In the following chapters we designed IMCUSUM, IMEWMA and CIM-VEWMA control charts to monitor an inverse *Maxwell* process and studied its' numerical performance with simulation and real-life study. Chapter 2 holds a detail literature survey. The next chapter contains a brief description of inverse *Maxwell* distribution and its' properties including characteristics function, survival function, hazard function and entropy. The development procedure of the cumulative sum control chart for inverse *Maxwell* distribution is described in Chapter 4. Here, the performance of the proposed chart is evaluated using of several run length properties including average run length (ARL), median of run length (MRL), standard deviation of run length (SDRL), performance comparison index (PCI), extra quadratic loss (EQL) and relative average run length (RARL). Comparisons of the proposed chart with the existing Shewhart type control chart named V_{IM} chart is also presented. Moreover here, we construct the proposed IMCUSUM chart for the simulated and real-life data set. In Chapter 5, we present the design structure of the exponentially weighted moving average control chart for inverse *Maxwell* distribution and describe a procedure to estimate the run length of our IMEWMA chart. It also contains the comparisons with some existing charts and some graphical presentations. In the same chapter, an illustrative example using simulated and real data are given for the practical necessity and suitability of the proposed chart. The design of the combined IM-VEWMA chart is discussed in in Chapter 6. The performance analysis as well as the comparative study has also been conducted along with the simulation and real-life example. Finally, the conclusions and recommendations are provided in Chapter 7.

CHAPTER TWO

LITERATURE RVIEW

In the recent years control charts become more popular among the industrial engineers that was in before. Most of the researchers proposed new types of control charts and analyzed several elementary run length characteristics of the control charts, for example, construction of V and V_{IM} charts for *Maxwell* and inverse *Maxwell* production process respectively. Practical application of the control charts has been shown by a few scholars. In the following section a detail literature of CUSUM control chart, EWMA control chart and Combined Shewhart-EWMA control chart are provided to get clear concept about their variation detecting ability and performing simplicity.

2.1 Literature review on CUSUM control chart

Cumulative sum control chart has been widely used by the researchers for monitoring both normal and non-normal production processes. To monitor the dispersion parameter of a normal process Acosta-Mejia et al. and Sanusi et al. introduced CUSUM charts while considering likelihood ratio and first-initial response respectively [28], [29]. Zhang et al. improve the performance of an adaptive CUSUM control chart by introducing an additional parameter over a range of mean variations while Shu et al. proposed similar chart for unknown mean shift [30], [31]. Castagliola et al. studied the run length properties of CUSUM chart for process variance [32]. Gan considered an exponentially distributed process and measure the relative performance of CUSUM chart for monitoring the rate of occurrences [33]. He also inspects the suitability of CUSUM control chart for monitoring the parameters of binomial distribution [34]. Taguchi's loss function is also implemented into CUSUM chart to optimize its performance [35]. Chowdhury et al. discussed the procedure for joint monitoring of parameters under nonparametric phase II samples [36]. Testik showed how to monitor the estimated parameters of Poisson process using CUSUM chart [37]. Recently, Hossain et al. proposed CUSUM chart for monitoring *Maxwell* process and visualizing its suitability over Shewhart type chart namely V chart [38].

2.2 Literature review on EWMA control chart

To diagnose normal production process more effectively and overcome the shortcoming of Shewhart chart Roberts proposed exponentially weighted moving average (EWMA) chart [39]. In recent years the EWMA chart is used to monitor the non-normal scheme. Borror

et al. constructed the EWMA chart for poisson distributed process [40]. In [41] Gan monitor the poisson observations through the EWMA chart and provide a real-life example. He also used EWMA chart to monitor observations generated from a binomial distribution [42]. Though its suitability to monitor a process Seyed et al. designed a chart named EWMA VSSI control chart for multivariate binominal observations [43]. EWMA chat is also constructed under negative binomial distribution to maintain the quality of a negative binomial process [44]. In order to deal with the non-normal process including skewed and heavy-tailed process Montgomery et al. provided an improved EWMA control chart [45]. Abbasi and Petros examine the applicability of the EWMA chart for dispersion in case of several non-normal distributions including logistic, student's t, Weibull, chi-square, exponential and gamma distribution and measure their performance [46] [47]. In [48], the EWMA chart is designed under the multivariate Student's t distribution and multivariate gamma distribution. To examine the censored lifetimes Raza and Zhang proposed EWMA chart under Poisson exponential distribution and Weibull distribution respectively [49] [50]. Under the assumption of Weibull distribution Arif et al. designed an EWMA control chart for failures truncated lifetime through with simulation study [51]. Most of the researchers use different run length properties such as average run length (ARL), standard deviation of run length (SDRL), median of run length (MRL) and percentile of run length (PRL) to examine the variations detecting ability of the control chart [52]. As a candidate of an overall performance measurement tool extra quadratic loss (EQL), relative average run length (RARL) and performance comparison index (PCI) are extensively applied in literature.

2.3 Literature review on Combined Shewhart-EWMA control chart

For enchaining and improving the shift detecting abilities different kinds of combined charts are available in literature. Combined Shewhart-EWMA (CSEWMA) and Combined Shewhart-CUSUM (CSCUSUM) control chart are developed by Lucas et al. and Westgard et al. respectively [53] [54]. Woodall and Mahmuod recommended for both univariate and multivariate cases that Shewhart chart should combine with EWMA chart [55]. Based on a simulation study Klein evaluated that CSEWMA control chart provide small ARL values than a lone Shewhart control chart [56]. Tolley et al. derived the cost function of CSEWMA chart and compare it with Shewhart chart [57]. An optimization technique to examine variations in the scheme mean by CSEWMA chart is presented by Simoes et al. [58]. Zhang et al. suggested to combine two or more EWMA charts namely composite EWMA chats

[59]. Abbas et al. applied the EWMA statistic as the input for CUSUM chart and defined this chart as mixed EWMA-CUSUM control chart [60]. Capizzi and Masarotto discussed the behavior of CSEWMA chart under the estimated parameters [61]. Morais and Pacheco discussed a combine CUSUM-Shewhart scheme under the assumption of binomial distribution and perform numerical comparison with one-sided CUSUM scheme [62]. For poisson counts, Abel derived one-sided combined Shewhart- CUSUM chart [63]. In case of binomial data, Elisa Henning et al. investigated the quality of combined Shewhart-CUSUM control chart and compare the shift diagnosing efficiency with individual Shewhart and CUSUM control chart [64].

2.4 Research questions

All the above discussed literature survey suggested us to consider the subsequent problems.

Problem 1: **Construct a CUSUM control chart under the assumption of inverse *Maxwell* distribution.**

CUSUM chart and its' various optimal types are usually implemented in literature for identifying variations under both normal and non-normal assumptions. Though its' performance is superior than any Shewhart type control chart but under the assumption of inverse *Maxwell* distribution it isn't developed yet. So, we have to construct CUSUM chart for inverse *Maxwell* distribution.

Problem 2: **Drive an EWMA control chart for inverse *Maxwell* distribution.**

From literature it is evident that EWMA control chart is widely used to monitor non-normal process but for inverse *Maxwell* distribution it is not defined yet. So, we need to propose the structure of EWMA control chart under inverse *Maxwell* distribution.

Problem 3: **Design a Combined EWMA-Shewhart control chart for inverse *Maxwell* distribution.**

Though different kinds of combined control charts are available in the literature to monitor production process but under the specific inverse *Maxwell* distribution it is not developed. So, we have to suggest a new combined type control chart for inverse *Maxwell* process by mixing the features of Shewhart and EWMA type control chart.

Problem 4: **Evaluate the numerical performance of the developed charts in industrial process monitoring.**

From literature we learn that the effectiveness of the control charts lies on how quickly they detect the variations from a process. Here, for our newly proposed control charts we will evaluate their shift detecting ability through various run length properties.

Problem 5: **Compare the proposed control charts with the existing chart in literature.**

In literature we know that the CUSUM and EWMA chart provide better performance than the Shewhart control chart whereas the combined chart is superior among these four control charts. Does this rule of thumb hold for the developed control charts? In this thesis, we will answer this question by comparing the charts performance.

Problem 6: **Application of the suggested charts in industrial process monitoring.**

There are no real-life applications of CUSUM, EWMA and Combined Shewhart-EWMA under inverse *Maxwell* distribution is available in the literature. So, we need to find out the applications.

CHAPTER THREE

INVERSE MAXEELL DITRIBUTION

In this chapter we will discuss the inverse *Maxwell* distribution. We will also introduce several characteristics of this inverse *Maxwell* distribution such as moment generating function, characteristics function, survival function, hazard function and mode. We also present estimation technique of population parameters for inverse *Maxwell* distribution. More specifically, maximum likelihood estimation is discussed. All these properties are derived by Arafat et al. [22].

3.1 Properties of inverse *Maxwell* distribution

The inverse *Maxwell* distribution derives its name from the renowned psychist and mathematician James Clark *Maxwell*. A continuous random variable R is said to have an inverse *Maxwell* distribution with parameter σ $(\sigma > 0)$ if its probability density function (PDF) is provided by

$$f(z,\sigma) = \sqrt{\frac{2}{\pi}}\,\sigma^{-3}r^{-4}e^{-\frac{1}{2r^2\sigma^2}}; r > 0. \tag{3.1}$$

The integral of the PDF defined above is 1, since it follows from the definition of the gamma function that

$$\int_0^\infty r^{n-1}e^{-r}dr = \Gamma(n). \tag{3.2}$$

The above-mentioned distribution has neither any shape nor location parameter but has only a scale parameter. The cumulative distribution function (CDF) of R is

$$F(r,\sigma) = \frac{2}{\sqrt{\pi}}\left[1 - \gamma\left(\frac{3}{2}, \frac{1}{2r^2\sigma^2}\right)\right]. \tag{3.3}$$

The following Figure 3.1 demonstrated the PDF and CDF of inverse *Maxwell* distribution with different values of the scale parameter. The figure visualize that the PDF and CDF are skewed and monotonic increasing respectively.

3.1.1 Moments of inverse *Maxwell* distribution

Theorem 3.1 The $s-th$ moments of inverse *Maxwell* distribution is given as

$$\mu_s' = \frac{2^{1-\frac{s}{2}}}{\sqrt{\pi}}\sigma^{-s}\Gamma\left(\frac{3-s}{2}\right). \tag{3.4}$$

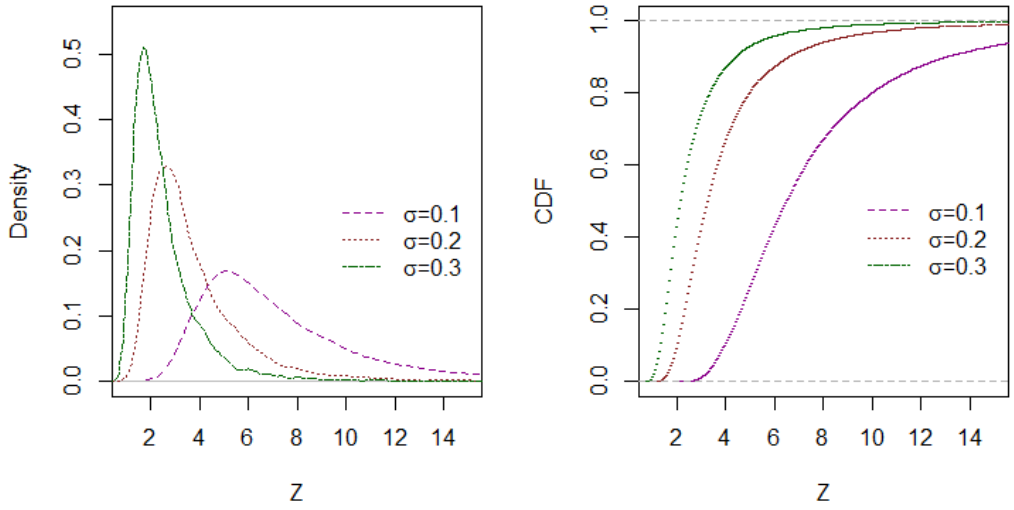

Figure 3.1: PDF and CDF of inverse *Maxwell* distribution for different value of parameter.

Proof. Recall equation (3.1) from [22] and equation (3.1) to gain the $s-th$ raw moment of inverse *Maxwell* distribution as

$$\mu_s' = E(R^s) = \int_0^\infty \sqrt{\frac{2}{\pi}}\, \sigma^{-3} r^{s-4} e^{-1/2r^2\sigma^2}\, dr.$$

Now, let $\frac{1}{2r^2\sigma^2} = u$ which means that $r = \sqrt{\frac{1}{2\sigma^2 u}}$. Performing differentiation on both sides with respect to u we get, $\frac{dr}{du} = -\frac{1}{2\sqrt{2}\sigma u^{\frac{3}{2}}}$. This can be written as $dr = -\frac{du}{2\sqrt{2}\sigma u^{\frac{3}{2}}}$. Limit becomes when $r = 0$ then $u = \infty$ and when $r = \infty$ then $u = 0$.

Hence,

$$\mu_s' = \sqrt{\frac{2}{\pi}}\sigma^{-3} \int_\infty^0 \left(\sqrt{\frac{1}{2\sigma^2 u}}\right)^{s-4} e^{-u} \frac{-1}{2\sqrt{2}\sigma u^{\frac{3}{2}}}\, du$$

$$= \frac{1}{\sqrt{\pi}} \int_0^\infty 2^{1-\frac{s}{2}} \sigma^{-s} e^{-u} u^{\frac{1}{2}-\frac{s}{2}}\, du$$

$$= \frac{2^{1-\frac{s}{2}}}{\sqrt{\pi}} \sigma^{-s} \int_0^\infty e^{-u}\, u^{\left(\frac{3}{2}-\frac{s}{2}\right)-1}\, du$$

$$= \frac{2^{1-\frac{s}{2}}}{\sqrt{\pi}} \sigma^{-s} \Gamma\left(\frac{3-s}{2}\right).$$

The above expressed equation evidently prove the theorem. □

Corollary 3.1 The first four raw moments of inverse *Maxwell* distribution are

$$\mu_1' = \sqrt{2/\pi}\sigma^{-1},$$

$$\mu_2' = \sigma^{-2},$$

$$\mu_3' = \left(\sqrt{2\pi}\right)^{-1}\sigma^{-3}, \text{and}$$

$$\mu_4' = \sigma^{-4}.$$

Proof. By substituting $s = 1, 2, 3$ and 4 in equation (3.4) the first four raw moments of inverse *Maxwell* distribution can be obtaining. □

Corollary 3.2 The 2nd, 3rd and 4th central moments of inverse *Maxwell* distribution are respectively,

$$\mu_2 = \left(\frac{\pi - 2}{\pi}\right)\sigma^{-2},$$

$$\mu_3 = \left(\frac{4-5\pi}{\sqrt{2}\pi\sqrt{\pi}}\right)\sigma^{-3}, \text{ and}$$

$$\mu_4 = \left(\frac{8\pi-\pi^2-12}{\pi^2}\right)\sigma^{-4}.$$

Proof. By adopting section 3.1.1 from [22] and putting the values of the raw moments in equation (3.4), (3.5) and (3.6) the desired central moments of inverse *Maxwell* distribution can be obtained. □

Corollary 3.3 The coefficient of skewness and kurtosis of inverse *Maxwell* distribution are

$$\beta_1 = \left(\frac{4-5\pi}{\sqrt{2}\pi\sqrt{\pi}}\right)^2 / \left(\frac{\pi-2}{\pi}\right)^3 \text{ and } \beta_2 = \left(\frac{8\pi-\pi^2-12}{\pi^2}\right) / \left(\frac{\pi-2}{\pi}\right)^2.$$

Proof. By putting the values of the raw moments in equation (3.5) the skewness and kurtosis of inverse *Maxwell* distribution can be obtaining. The required formula is given as

$$\beta_1 = \frac{\mu_3^2}{\mu_2^3} \text{ and } \beta_2 = \frac{\mu_4}{\mu_2^2}. \tag{3.5}$$

3.1.2 MGF of inverse *Maxwell* distribution

Theorem 3.2 The moment generating function for inverse *Maxwell* distribution is

$$M_R(t) = \sum_{s=0}^{\infty} \frac{t^s}{s!} \frac{2^{1-\frac{s}{2}}}{\sqrt{\pi}} \sigma^{-s} \Gamma\left(\frac{3-s}{2}\right). \tag{3.6}$$

Proof. Recalling equation (3.7) from [22] and in that equation put the value of μ_s' from equation (3.4), then we will get our desired moment generating function of the inverse *Maxwell* distribution.

Hence, prove. □

3.1.3 CF of inverse *Maxwell* distribution

Theorem 3.3 The characteristics function for inverse *Maxwell* distribution is

$$\phi_R(t) = \sum_{s=0}^{\infty} \frac{(it)^s}{s!} \frac{2^{1-\frac{s}{2}}}{\sqrt{\pi}} \sigma^{-s} \Gamma\left(\frac{3-s}{2}\right). \tag{3.7}$$

Proof. Recalling equation (3.11) from [22] and in that equation put the value of μ_s' from equation (3.4), then we will get our desired CF of the inverse *Maxwell* distribution.

Hence, prove. □

3.1.4 Survival function of inverse *Maxwell* distribution

Theorem 3.4 Survival function of inverse *Maxwell* distribution is given as

$$S(t) = 1 - \frac{2}{\sqrt{\pi}} \left[1 - \gamma\left(\frac{3}{2}, \frac{1}{2r^2\sigma^2}\right)\right]. \tag{3.8}$$

Proof. Using definition given in equation (3.13) from [22] and the CDF given in equation (3.3) we get the result given in equation (3.8). □

3.1.5 Hazard function of inverse *Maxwell* distribution

Theorem 3.5 Hazard function of inverse *Maxwell* distribution is given as

$$h(t) = \sqrt{\frac{2}{\pi}}\, \sigma^{-3} r^{-4} e^{-1/2r^2\sigma^2} / 1 - \frac{2}{\sqrt{\pi}} \left[1 - \gamma\left(\frac{3}{2}, \frac{1}{2r^2\sigma^2}\right)\right]. \tag{3.9}$$

Proof. Using definition equation (3.14) in [22] and equation (3.1) and (3.8) we put the value of PDF and survival function then we will get the result in equation (3.9). □

3.1.6 Mode of inverse *Maxwell* distribution

Theorem 3.6 If the PDF of the inverse *Maxwell* distribution is according to equation (3.1) then the mode of the distribution is $\frac{1}{2\sigma}$.

Proof. Recalling the relationships given in equation (3.15) from [22] and differentiate equation (3.1) with respect to r and putting is equal to zero. We get,

$$f(r)' = \sqrt{\frac{2}{\pi}}\,\sigma^{-3}\left(\frac{d}{dr}(r^{-4})e^{-\frac{1}{2r^2\sigma^2}} + \frac{d}{dr}\left(e^{-\frac{1}{2r^2\sigma^2}}\right)r^{-4}\right)$$

$$= \frac{\sqrt{2}\left(-4e^{-\frac{1}{2r^2\sigma^2}}r^2\sigma^2 + e^{-\frac{1}{2r^2\sigma^2}}\right)}{\sqrt{\pi}\sigma^5 r^7}$$

$$= \frac{(1-4r^2\sigma^2)}{r^3\sigma^2}\,f(r)$$

Now, we can write,

$f(r)' = 0$

$\Rightarrow \frac{(1-4r^2\sigma^2)}{r^3\sigma^2} = 0$ [Since $f(r) \neq 0$]

$\Rightarrow r = \frac{1}{2\sigma}$.

Therefore, $r = \frac{1}{2\sigma}$ is the mode of the distribution. □

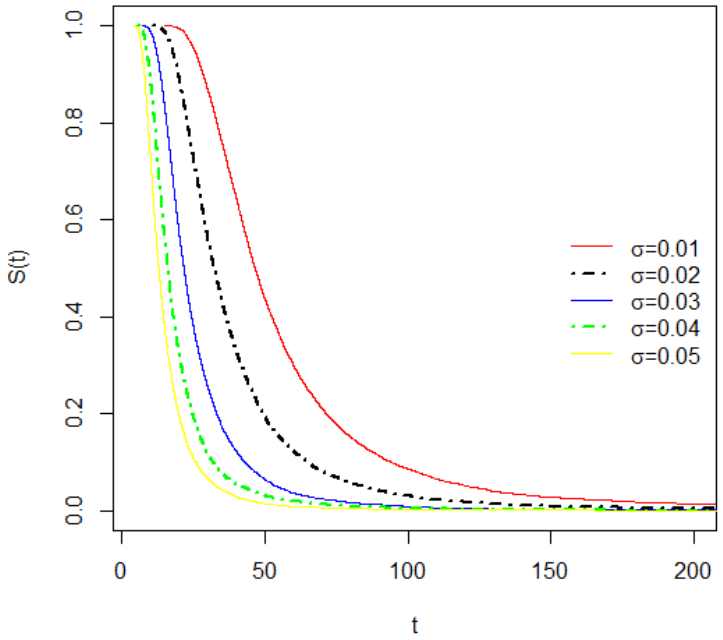

Figure 3.2: The Survival curve of inverse *Maxwell* distribution for different value of parameter.

3.2 MLE of the parameter of inverse *Maxwell* distribution

For a sample of size n, consider a set of observations to be $r_1, r_2 \ldots . r_n$ with pdf $f(r_1, \sigma), f(r_2, \sigma), \ldots \ldots f(r_n, \sigma)$. Then according to the section 4.1 in [22], the likelihood function is given by,

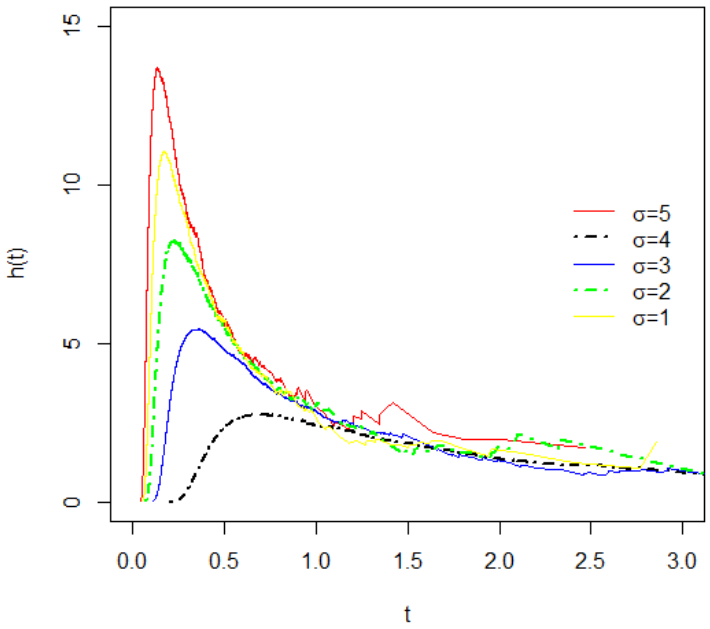

Figure 3.3: The Hazard curve of inverse *Maxwell* distribution for different value of parameter.

$$L(\sigma, r) = \left(\sqrt{\frac{2}{\pi}}\sigma^{-3}\right)^n \prod_{i=1}^{n} r_i^{-4} e^{-\sum_{i=1}^{n}\frac{1}{2r_i^2\sigma^2}}$$

Now the log-likelihood function becomes,

$$log(L) = nlog\sqrt{\frac{2}{\pi}} - 3nlog(\sigma) + \sum_{i=1}^{n} log(r_i^{-4}) - \sum_{i=1}^{n}\frac{1}{2r_i^2\sigma^2} \qquad (3.10)$$

Differentiating equation (3.10) with respect to parameter σ and then equating to zero. We get,

$$\frac{\partial}{\partial\sigma} log(L) = 0$$

$$\Rightarrow -\frac{3n}{\sigma} + \sum_{i=1}^{n}\frac{2}{2r_i^2\sigma^3} = 0$$

$$\Rightarrow \frac{3n}{\sigma} = \sum_{i=1}^{n}\frac{1}{r_i^2\sigma^3}$$

$$\Rightarrow \sigma^2 = (3n)^{-1} \sum_{i=1}^{n} \frac{1}{r_i^2}.$$

Finally, the MLE of σ is given by,

$$\hat{\sigma} = \sqrt{(3n)^{-1} \sum_{i=1}^{n} \frac{1}{r_i^2}} \ . \tag{3.11}$$

3.3 Summary of the inverse *Maxwell* distribution

In this chapter, we introduce an ordinary inverse *Maxwell* distribution. We discussed several characteristics of the distribution. The mentionable characteristics of the distribution are MGF, CF, survival function, hazard function, mode and entropy. We show the functional form of the MGF and CF. Due to the importance of studying the shape characteristics of a distribution, we visualize first four raw and central moments for the inverse *Maxwell* distribution. From this moment we estimate the skewness and kurtosis of the desired distribution. In statistical analysis estimation serves a vital role. Here we estimate the parameter of the inverse *Maxwell* distribution by MLE.

It is always expected to have an application for any newly developed method in order to proof its significance. Therefore, in the next chapters, the application of inverse *Maxwell* distribution has been provided in the field named as statistical process control.

CHAPTER FOUR

IMCUSUM CONTROL CHART

In 1954, Page proposed cumulative sum control chart as a member of memory type control chart, from the beginning this chart has been regularly implemented under normal distribution for monitoring process location and scale parameters [65]. In this chapter, we will introduce this chart namely IMCUSUM control chart because it will work under the assumption of inverse *Maxwell* distribution. After the suitability of this proposed chart will be monitored as well as the comparison and application will be visualized.

4.1 Construction of the IMCUSUM control chart

Let us consider a random variable R where $R = 1/2Y^2\sigma^2$ and the probability density function of this random variable is given as

$$f_R(r) = \frac{1}{\Gamma\left(\frac{3}{2}\right)} r^{\frac{3}{2}-1} e^{-r}, \tag{4.1}$$

which is the PDF of *gamma* distribution with parameter $3/2$ and 1 [22]. We know that the additive property of the gamma distribution is if P_i is a random variable that follows gamma distribution with parameter α_i and β then for n samples, $\sum_{i=1}^{n} p_i \sim gamma\ (\sum_{i=1}^{n} \alpha_i, \beta)$. For our case, $r = \frac{1}{2y^2\sigma^2} \sim gamma(3/2,1)$ then $\sum_{i=1}^{n} r_i \sim gamma\left(\frac{3n}{2}, 1\right)$. Consider another random variable V_{IM} which is the square of MLE estimator of the scale parameter σ and we will use it to derive a pivotal quantity namely T. This pivotal quantity has a gamma distribution with parameter $3n/2$ and 1, where $T = 3nV_{IM}/2\sigma^2$. So, T is a gamma random variable with same mean and variance, $\frac{3n}{2}$. The random variable V_{IM} has a relationship with the pivotal quantity T from that relation the mean and variance of V_{IM} are derived as $E[V_{IM}] = \sigma^2$ and $Var(V_{IM}) = \frac{2\sigma^4}{3n}$ respectively [22]. Now, by using the jacobian transformation $J(t \to v_{IM}) = \frac{3n}{2\sigma^2}$, the density function of V_{IM} can be written as

$$f(v_{IM}) = \frac{1}{\Gamma\left(\frac{3n}{2}\right)\left(\frac{2\sigma^2}{3n}\right)^{\frac{3n}{2}}} (v_{IM})^{\frac{3n}{2}-1} e^{-\left(\frac{v_{IM}}{\frac{2\sigma^2}{3n}}\right)}. \tag{4.2}$$

The density of the random variable V_{IM} is a member of the exponential family of distributions, so according Hawkins et al. [3] for the construction of CUSUM control chart

under the assumptions of inverse *Maxwell* distribution, the distribution of V_{IM} can be expressed as

$$f(v_{IM}) = \exp\left(-\frac{v_{IM}}{\frac{2\sigma^2}{3n}} + \left(\frac{3n}{2} - 1\right)\ln(v_{IM}) - \frac{3n}{2}\ln\frac{2\sigma^2}{3n} - \ln\left(\Gamma\frac{3n}{2}\right)\right). \quad (4.3)$$

The plotting statistic of the CUSUM control chart statistic for monitoring a scale parameter is given as and

$$C_i^+ = \max[0, V_{IM_i} - k + C_{i-1}^+] \ , \quad (4.4)$$

$$C_i^- = \min[0, V_{IM_i} + k + C_{i-1}^-], \quad (4.5)$$

where k is the reference parameter and we assume Where $C_0^+ = C_0^- = 0$. Since our proposed chart will work for a non-normal distribution so, we have to estimate the reference in a different approach. From equation (4.2), we know that the distribution of V_{IM} is a special form of gamma distribution so by comparing with the gamma CUSUM chart, the reference value for our proposed IMCUSUM chart can be expressed as $k = -\frac{\ln\sigma_1^2 - \ln\sigma_0^2}{(\sigma_1^{-2} - \sigma_0^{-2})} = -\frac{\ln(\delta)}{(\sigma_1^{-2} - \sigma_0^{-2})}$.

In this thesis, we consider the upper-sided control chart because Hossain et al. [38] reported that increase in variation is mostly disadvantage than decrease in variation, under the following hypothesis

$H_0: \sigma^2 = \sigma_0^2$; or, $\delta = 1$, i.e. No shift occurs in the process,

$H_1: \sigma^2 = \sigma_1^2 = \delta\sigma_0^2$; or, $\delta \neq 1$, i.e. Shift occurs in the process.

Here, δ denotes the shift in the process. It is to be mentioned that when the null hypothesis is true, that is $\delta = 1$, k will be zero. We assume the control limit, h for an in-control situation where $C_i^+ < h$ by setting a specific in-control average run length, $ARL_0 = 370$. Here, h is defined as upper control limit.

Remark: Hawkins et al. [3] reported that the null hypothesis of CUSUM control chart will never be accepted when the process is in control due to this reason we assume a small amount of variations when we are in control hence we can accept that.

4.3 Performance Measures

To access the statistical performance of our proposed control chart, we studied several run length properties named as average run length (ARL), standard deviation of run length (SDRL) and median of run length (MRL). There are three ways to estimate the run length of control chart, the integral equation method, the Markov chain approach and Monte Carlo simulation method [66]. We used Monte Carlo simulation method and assume that an in-control process follows an inverse *Maxwell* distribution with $\sigma_0 = 8.810865 \times 10^{-5}$. In R 3.3.4 a simulation study has been conducted to estimate the run lengths. We consider three different sample sizes, $n = 3,6$ and 9 as well as the process contains 10% of variations when it is in-control situation. The performance of the proposed chart is investigated for different shift sizes say $\delta = 1.00, 1.10, 1.25, 1.50, 1.75, 2.00, 2.5$ and 3. The following tables, the estimated values are provided.

Table 4.1: ARL, SDRL and MRL of IMCUSUM chart for different n with $k = 8.14 \times 10^{-9}$ and $\sigma_0 = 8.810865 \times 10^{-5}$ at $ARL_0 \cong 370$.

Sample size (n)									
	3			6			9		
δ	ARL	$SDRL$	$MDRL$	ARL	$SDRL$	$MDRL$	ARL	$SDRL$	$MDRL$
1.00	371.21	370.22	279	370.31	371.24	280	373.86	369.96	272
1.05	132.75	102.33	126	116.73	92.71	118	94.63	66.39	94
1.10	83.19	57.30	83	48.85	30.59	67	35.52	23.25	58
1.15	49.91	38.35	57	37.55	23.57	41	26.17	12.37	29
1.20	37.93	20.79	36	20.08	11.51	27	17.87	7.79	19
1.25	30.27	15.95	14	16.88	6.04	9	10.95	5.73	7
1.35	26.38	13.39	11	14.24	5.73	8	8.67	3.35	5
1.50	12.26	5.34	8	7.45	3.16	6	4.18	2.06	3
1.75	8.38	3.85	4	5.24	2.95	2	4.11	1.35	1
2.00	7.21	2.86	3	4.94	1.50	2	3.09	0.90	1

The ARL is enumerated at a specific shift point because of this Wu et al. have raised concern about the suitability of ARL for measuring performance of control charts [67]. Consequently, we further use some overall performance measuring tools like as extra quadratic loss (EQL), relative average run length (RARL) and performance comparison index (PCI). Below is a brief description of required measures.

$$EQL = \frac{1}{\delta_{max}-\delta_{min}} \int_{\delta_{min}}^{\delta_{max}} \delta^2 ARL(\delta) d\delta \ ,$$

$$RARL = \frac{1}{\delta_{max}-\delta_{min}} \int_{\delta_{min}}^{\delta_{max}} \frac{ARL(\delta)}{ARL_{benchmark}(\delta)} d\delta \ \text{ and } PCI = \frac{EQL}{EQL_{benchmark}},$$

where E stands for the expected value, $ARL(\delta)$ is the ARL of a particular chart at shift δ, δ_{min} and δ_{max} are the minimum and maximum values of the shift, $ARL_{benchmark}(\delta)$ and $EQL_{benchmark}$ are the ARL and EQL of the best chart at δ respectively. The smaller values for these measures are expected. For the benchmark chart, we consider the value of RARL and PCI equal to one and for other charts it is more than one [68]. The values of these overall performance measures are mentioned in Table 4.3. Based on Table 4.1, Table 4.3 and Figure 4.1, we can advocate the following conclusions:

1. The average run length (ARL) is always approximately equal to ARL_0 (i.e. in-control ARL) for any choice of shift, δ which implies that IMCUSUM chart is constructed without any erroneous effect (cf. Table 4.1).
2. For an in-control process, the SDRL values and the corresponding ARL values for any sample size, n are approximately equal. For example: The ARL and SDRL values are 371.21 and 370.22 respectively at $n = 3$. (cf. Tables 4.1).
3. In case of average run length, the waiting number of samples are decreasing as the shift increases in the process scale parameter. For example: At 15% increment of shift the waiting number of sample is approximately 50 for sample size 3 and it will declined to 13 samples where the sample size is fixed but the shift is increased by 50%. Similarly, if we take sample size 9 then at 5% variations the waiting number of sample is 94 and for 35% variations it is only approximately 8. (cf. Tables 4.1).
4. The SDRL values rapidly decrease as the shift increases in the process. For example: At 5% increment of shift the SDRL is 102.33 for $n = 3$ and under same parameters at 50% increment of shift the SDRL becomes 12.26.
5. The ARL and SDRL values are not proportional to each other (cf. Tables 4.1 and above mentioned two properties).

6. The run length distribution of the IMCUSUM chart is positively skewed because for both in and out of control situations and under any sample size, the ARL values are greater than the MRL values. For example: when $n = 6$ and $\delta = 1.5$ the ARL and MRL values are 7.45 and 6 respectively. Also, for $n = 9$ and $\delta = 2$, the ARL and MRL values are 3.09 and 1 correspondingly (cf. Tables 4.1).
7. The proposed chart is more sensitive to small shifts but for detecting large shifts it is not that much worthy. It is observed in Figure 4.1.
8. Based on the overall performance values of the proposed chart and Table 4.1, we conclude that our process chart is suitable for detecting variations of an inverse *Maxwell* distributed process.

4.4 Comparative Analysis

In this section, we compare our proposed memory type control chart with the exiting control chart which is available in the literature for monitoring an inverse *Maxwell* process. Till now, only a Shewhart type control chart is available which is usually used for large variations. To evince the comparison we analyze the shift specific run length properties as well as the overall run length properties. Table 4.2 exhibits that the in-control ARL of the proposed chart and V_{IM} chart are same. As the shift increases the ARL decreases for both cases but the rate of decrement defers which is our out point of interest. For 5% increment of shift, the ARLs of IMCUSUM and V_{IM} chart are 287.01 and 116.73 respectively as well as the average run lengths are 31.54 and 14.24 when the variations are increased by 35%. This suggest that the newly proposed chart can detect small amount shift more quickly than the V_{IM} control chart. From an in-control situation to out-of-control situation the ARL is decreased by 89% for 50% arise of shift under the Shewhart type control chart whereas almost 98% out of control signals are detected by our newly proposed IMCUSUM control chart for the same increment of variation. Though the performance of IMCUSUM chart is superior to V_{IM} chart for small amount of shift but it is not up to mark for monitoring large variations. For example, at 100% increment of shift the ARL of IMCUSUM chart is greater than the existing chart. Figure 4.1 also visualizes the sharp fall of average run length of IMCUSUM chart for small shift and overlapping and downward trend for large variations with V_{IM} chart. Though the ARL comparative analysis is based on specific shift so, we consider some overall variations run length properties including extra quadratic loss (EQL), relative average run length (RARL) and performance comparison index (PCI). The values of all these three tools are all for IMCUSUM chart than the V_{IM} chart. Such that, the EQL

is 37.63 and 79.52 for IMCUSUM and V_{IM} control chart respectively. Further values of these tolls are available in Table 4.3. Finally, we can conclude that the IMCUSUM control chart should be implemented for monitoring an inverse *Maxwell* distributed process, especially for small and moderate amount of variations.

Table 4.2: ARL for IMCUSUM and V_{IM} chart at $ARL_0 \cong 370$ with $n = 6$.

Chart \ δ	1.00	1.05	1.10	1.15	1.20	1.25	1.35	1.50	1.75	2.00
V_{IM}	373.32	287.01	202.79	130.73	88.22	61.22	31.54	14.58	5.86	3.39
IMCUSUM	370.31	116.73	48.85	37.55	20.08	16.88	14.24	7.45	5.24	4.94

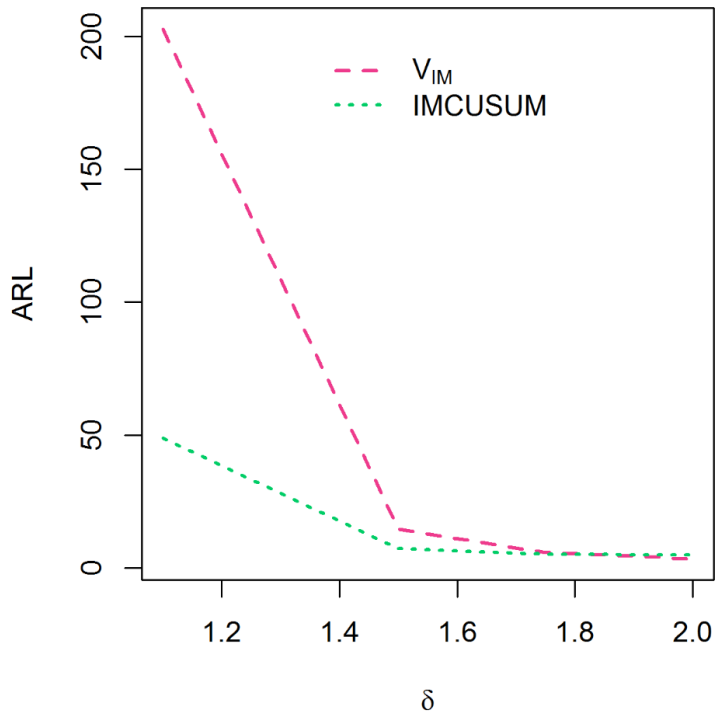

Figure 4.1: ARL curves for IMCUSUM and V_{IM} chart at $n = 6$.

4.5 Application of IMCUSUM Chart in Real-life

Different kinds of data such as lifetime data, time series data and genetic data may follow inverse *Maxwell* distribution. To highlight the pertinence of these control charts with real data, we use the car brake pedal lifetime data which is found in Lawless [69].This data set is the left front brake pads lifetime on a sample of 98 vehicles and these are odometer readings.

To inspect whether the data set follow inverse *Maxwell* distribution or not according to the K-S test the null hypothesis is that the data set comes from inverse *Maxwell* distribution

and the alternative hypothesis is that data set doesn't come from inverse *Maxwell* distribution. For our data set the K-S test statistic value is 0.105 where at 1% level of significance the critical value is 0.144 the p value is 0.452. Clearly the calculated value is less than the tabulated value of K-S test statistic and p value is larger than the level of significance, so we cannot reject the null hypothesis that the data follows inverse *Maxwell* distribution.

Table 4.3: EQL, RARL and PCI of RL of IMCUSUM and V_{IM} chart for different λ at $ARL_0 \cong 370$.

Control Chart	EQL	RARL	PCI
IMCUSUM	37.63	1	1
V_{IM}	79.52	2.05	2.11

The lifetime in kilometers are as follows:

Table 4.4: Lifetime of car's brake pad (in km).

Sample Number	Observations			Sample Number	Observations			Sample Number	Observations		
	1st	2nd	3rd		1st	2nd	3rd		1st	2nd	3rd
1	46.8	50.8	68.8	9	53.9	43.4	44.8	17	79.4	43.4	81.6
2	110	79.4	49.2	10	42.4	95.7	46.7	18	100.6	50.5	54.0
3	50.5	52.0	45.2	11	83.6	83.0	42.4	19	55.0	77.2	42.4
4	89.5	92.5	61.9	12	54.0	78.1	165.5	20	54.9	72.8	77.6
5	55.0	89.1	82.6	13	49.8	92.6	68.9	21	74.7	72.2	143.6
6	92.5	82.6	49.8	14	55	88.0	82.6	22	69.6	124.6	83.6
7	79.4	88.0	83.6	15	103.6	55.0	72.2	23	92.5	49.8	68.8
8	54.0	49.2	92.5	16	42.4	45.2	83	24	110	124.6	74.8

Thus, we adopt this data to develop control chart for inverse *Maxwell* parameter. After truncation the data consists of car brake pad's lifetime with 72 observations. We considered the data in the form of subgroups, each of size 3, that results into 24 subgroups. Then we use the subgroups further in the establishment of the control charts.

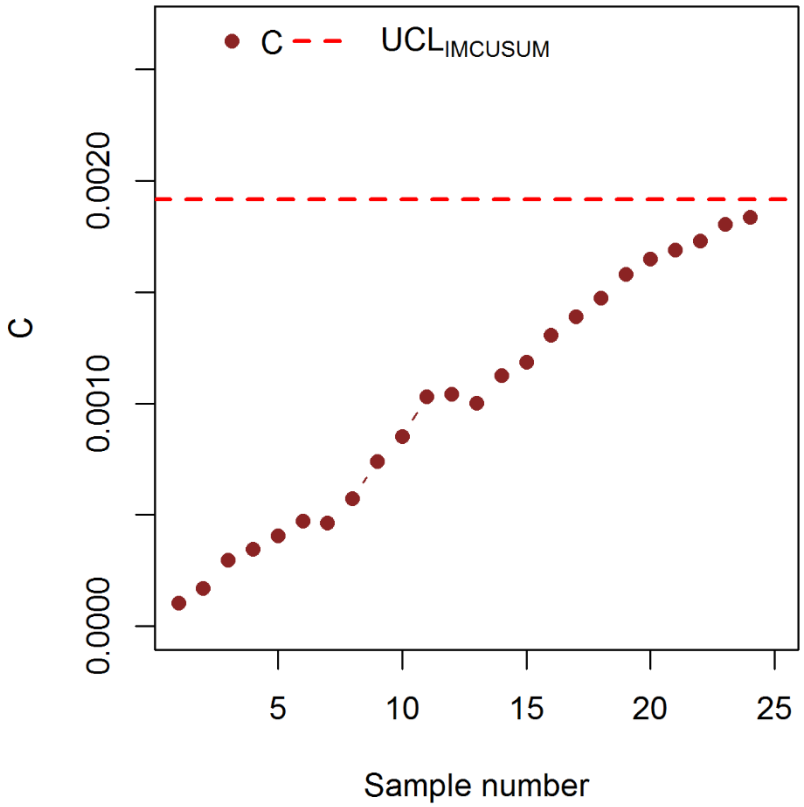

Figure 4.2: IMCUSUM chart for cars' brake pad lifetime at $\delta = 1$.

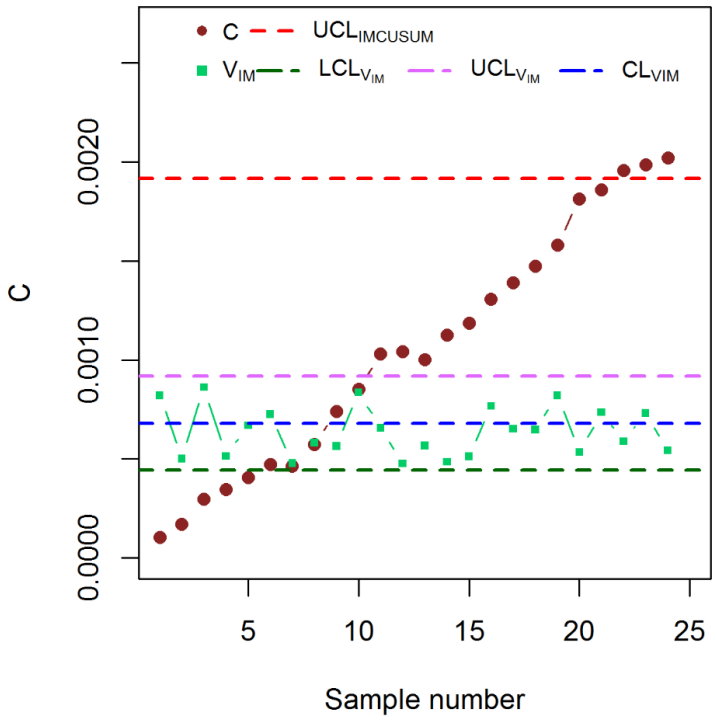

Figure 4.3: IMCUUSM and V_{IM} chart for cars' brake pad lifetime at $\delta = 1.15$ (after 19th sample).

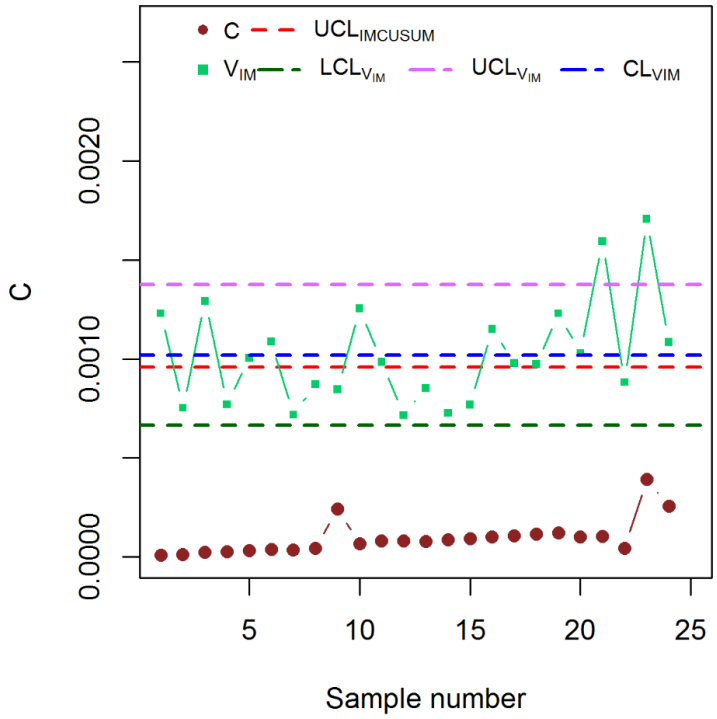

Figure 4.4: IMCUUSM and V_{IM} chart for cars' brake pad lifetime at $\delta = 3.75$ (after 19th sample).

Now we fabricate the control chat for IMCUSUM using the descripted procedure in section 4.1. For our given data, the estimated value of the MLE is $\bar{V}_{IM} = 8.77915 \times 10^{-5}$ and we consider this as σ. The IMCUSUM chart in Figure 4.2 is constructed to check whether it can identify an in-control process or not. For, this procedure we consider the reference parameter $k = 9.954 \times 10^{-9}$ and it provides an upper control limit $h = 9.579 \times 10^{-4}$ at $ARL_0 = 370$. Figure 4.2 evinces that all the plotting statistic lies with the control limit thus, our proposed control chart is performing well. Now, we can check whether it can detect an out-of-control situation or not. For this purpose, we construct the IMCUSUM chart and V_{IM} chart in a single figure and intentionally increase the shift by 15% after 19th sample which advocated that the last 5 samples contains 15% variations. From Figure 4.3, it is evident that our proposed chart can successfully detect 3 out of control samples among 5 while the existing V_{IM} chart is failed to identify any out-of-control samples.

Now. We increase the shift and consider $\delta = 3.75$ which means the last 5 samples of an inverse *Maxwell* process contains 275% variations among 24 samples. Orthodoxly, we observe that the IMCUSUM chart can't identify any out of control samples but the Shewhart type V_{IM} chart clearly detect 2 samples out of 5 samples (cf. Figure 4.4). Finally,

this advocates that our proposed chart is superior than the existing counter parts for monitoring small amount of variations and its' performance isn't up to mark for detecting large variations comparing to V_{IM} chart.

4.6 Summary of the Proposed Chart

Control charts are usually used to identify shift from an out-of-control process as quick as possible whether the process is normally distributed or not. In industry, the most challenging task is to detect small variations from a non-normal process. To accomplish this task, in this chapter, we propose a memory type control chart namely IMCUSUM chart for an inverse *Maxwell* distributed process. The performance of this control chart is evaluated through several shift specific and overall run length properties including average run length, median run length and extra quadratic loss along with relative average run length. The comparative analysis with the existing V_{IM} control chart suggest that the proposed chart is very sensitive to small variations rather than large shifts and a real-life example provides its' significance for monitoring an inverse *Maxwell* process to detect small variations. In the following chapter, we will introduce another memory type control chart namely IMEWMA control chart under the similar assumptions.

CHAPTER FIVE

IMEWMA CONTROL CHART

Memory type control charts are widely implied to identify small and moderate assignable cause variations of scale parameter σ in process monitoring. As a candidate of memory type control chart, Roberts developed the exponentially weighted moving average control chart [39]. This chart works under the normality assumption for this we introduce a new EWMA chart on the basis of non-normal distribution. In our case the asymmetric distribution is inverse *Maxwell* distribution and we denote our proposed chart as IMEWMA chart. In this chapter the development procedure of the IMEWMA chart is presented in the following texts.

5.1 Design of the IMEWMA control chart

Let us consider a random variable R where $R = 1/2Y^2\sigma^2$ and the probability density function of this random variable is given in equation (3.1) which is the PDF of *gamma* distribution with parameter $3/2$ and 1 [22].We know that if U_i is a random variable that follows a gamma distribution with parameter α_i and β then for n samples, $\sum_{i=1}^{n} U_i \sim gamma\,(\sum_{i=1}^{n}\alpha_i, \beta)$. For our case, if $R = \frac{1}{2Y^2\sigma^2} \sim gamma(3/2,1)$ then $\sum_{i=1}^{n} R_i \sim gamma\left(\frac{3n}{2}, 1\right)$. We will use another random variable V_{IM} such that $V_{IM} = (3n)^{-1}\sum_{i=1}^{n}\frac{1}{Y_i^2}$, which is the square of MLE estimator of the scale parameter σ to derive a pivotal quantity T. This pivotal quantity has a gamma distribution with parameter $3n/2$ and 1, where $T = 3nV_{IM}/2\sigma^2$. So, T is a gamma random variable with same mean and variance, $\frac{3n}{2}$. The random variable V_{IM} has a relationship with the pivotal quantity T ; thus, the mean and variance of V_{IM} are derived as $E[V_{IM}] = \sigma^2$ and $Var(V_{IM}) = \frac{2\sigma^4}{3n}$ respectively.

The statistic which is usually plotted in the EWMA control chart is a weighted merger of the present and previous fact. It is expressed as

$$Z_i = \lambda V_{IM_i} + (1-\lambda)Z_{i-1}, \tag{5.1}$$

where V_{IM_i} is the present observation (for i=1,2,3,…), Z_{i-1} is the previous facts about the scale parameter. The smoothing constant (λ) is lying between 0 and 1 (i.e. $0 < \lambda \leq 1$). An alter form of the EWMA statistic given in (5.1) can be presented as

$$Z_i = \sum_{J=0}^{i-1} \lambda(1-\lambda)^j V_{IM_{i-j}} + (1-\lambda)^j Z_0. \tag{5.2}$$

The weights $\lambda(1-\lambda)^j$ in (5.2) decrease exponentially as the sample observations become more previous. For $\lambda = 1$, the IMEWMA control chart becomes equivalent to the V_{IM} chart. The initial value, Z_0, is taken to be equal to σ_0^2. If we do not have information available about the target scale parameter, then it can be estimated from Phase I samples. The mean and variance of the IMEWMA statistic are given as

$$Mean(Z_i) = \sigma^2 \,, Variance(Z_i) = \frac{2\sigma^4}{3n}\left\{\frac{\lambda}{2-\lambda}\left(1-(1-\lambda)^{2i}\right)\right\}, \tag{5.3}$$

where σ^2 is the square of the process scale parameter. Based on the above results, the control structure of an IMEWMA chart is given as

$$LCL = W_1\sigma^2, CL = \sigma^2 \text{ and } UCL = W_2\sigma^2, \tag{5.4}$$

where, $W_1 = \left[1 - L\sqrt{\frac{2}{3n} \times \frac{\lambda}{2-\lambda}(1-(1-\lambda)^{2i})}\right]$ and

$W_2 = \left[1 + L\sqrt{\frac{2}{3n} \times \frac{\lambda}{2-\lambda}(1-(1-\lambda)^{2i})}\right]$.

In real-life scenario two situations appear in process monitoring of the inverse *Maxwell* scale parameter: i) σ^2 known and ii) σ^2 unknown. In case of known σ^2, the limits can be written as

$$LCL = W_1\sigma_0^2; \qquad CL = \sigma_0^2 \quad \text{and} \qquad UCL = W_2\sigma_0^2.$$

But in case of unknown σ^2, we estimate V_{IM} and use it as follows:

$$LCL = W_1\bar{V}_{IM}; \qquad CL = \bar{V}_{IM} \quad \text{and} \qquad UCL = W_2\bar{V}_{IM}.$$

The factor L is obtained using Monte Carlo Simulation with $\sigma_0 = 8.810865 \times 10^{-5}$ in such a way that the expected in control ARL (ARL_0) has been obtained. L fixes the spread of the control limits and its value is chosen according to the choice of the ARL_0.

Table 5.1 represents L coefficients which is used to calculate the factors W_1 and W_2. The L coefficients are estimated by using the following algorithm:

Step 1: Specify an in control average run length (ARL_0) value. In our case, we consider 370.

Step 2: The value L is obtained such that $ARL_0 \geq 370$.

Table 5.1: L coefficients.

Sample Size (n)	In control Average Run Length ($ARL_0 \cong 370$)			
	$\lambda = 0.05$	$\lambda = 0.25$	$\lambda = 0.50$	$\lambda = 0.75$
	L			
2	2.531	3.269	3.728	3.970
3	2.523	3.164	3.558	3.764
5	2.528	3.064	3.376	3.550
6	2.528	3.031	3.321	3.472
7	2.521	3.011	3.291	3.426
9	2.517	2.987	3.216	3.353
10	2.516	2.977	3.190	3.309
12	2.514	2.967	3.152	3.279

Table 5.2: Factor for IMEWMA control Chart for inverse *Maxwell* parameter for $\lambda = 0.05$ and $ARL_0 \cong 370$.

Time (i)	Sample Size (n)					
	3		6		9	
	W_1	W_2	W_1	W_2	W_1	W_2
1	0.9404	1.0596	0.9579	1.0421	0.95657	1.0342
2	0.9177	1.0822	0.9420	1.0580	0.9528	1.0472
4	0.8892	1.1108	0.9218	1.0782	0.9390	1.0636
6	0.8705	1.1295	0.9087	1.0913	0.9364	1.0744
8	0.8571	1.1425	0.8992	1.0080	0.9179	1.0821
10	0.8470	1.1527	0.8921	1.1079	0.9121	1.0879
15	0.8375	1.1692	0.8806	1.1194	0.9028	1.0972

Table 5.3: Factor for IMEWMA control Chart for inverse *Maxwell* parameter for $\lambda = 0.25$ and $ARL_0 \cong 370$.

Time (i)	Sample Size (n)					
	3		6		9	
	W_1	W_2	W_1	W_2	W_1	W_2
1	0.6271	1.3728	0.7482	1.2518	0.7967	1.2032
2	0.5339	1.4661	0.6853	1.3147	0.7460	1.2540
4	0.4652	1.5348	0.6389	1.3611	0.7085	1.2915
6	0.4453	1.5547	0.6255	1.3745	0.6976	1.3024
8	0.4391	1.5609	0.6213	1.3787	0.6943	1.3057
10	0.4372	1.5628	0.6199	1.3800	0.6932	1.3067
15	0.4363	1.5637	0.6194	1.3806	0.6928	1.3072

Table 5.4: Factor for IMEWMA control Chart for inverse *Maxwell* parameter for $\lambda = 0.50$ and $ARL_0 \cong 370$.

Time (i)	Sample Size (n)					
	3		6		9	
	W_1	W_2	W_1	W_2	W_1	W_2
1	0.1614	1.8386	0.4465	1.5535	0.5623	1.4376
2	0.0624	1.9376	0.3812	1.6188	0.5107	1.4893
4	0.0335	1.9664	0.3621	1.6379	0.4956	1.5043
6	0.0317	1.9682	0.3609	1.6391	0.4947	1.5053
8	0.0316	1.9684	0.3609	1.6391	0.4947	1.5053
10	0.0316	1.9684	0.3609	1.6391	0.4947	1.5053
15	0.0316	1.9684	0.3606	1.6391	0.4947	1.5053

Table 5.5: Factor for IMEWMA control Chart for inverse *Maxwell* parameter for $\lambda = 0.75$ and $ARL_0 \cong 370$.

Time (i)	Sample Size (n)					
	3		6		9	
	W_1	W_2	W_1	W_2	W_1	W_2
1	0	2.3368	0.1332	1.8667	0.3148	1.6852
2	0	2.3779	0.1066	1.8934	0.2937	1.7063
4	0	2.3806	0.1048	1.8952	0.2923	1.7077
6	0	2.3806	0.1048	1.8952	0.2923	1.7077
8	0	2.3806	0.1048	1.8952	0.2923	1.7077
10	0	2.3806	0.1048	1.8952	0.2923	1.7077
15	0	2.3806	0.1048	1.8952	0.2923	1.7077

In addition, Tables 5.2, 5.3, 5.4 and 5.5 display the corresponding $W_1$and W_2 factors for different values of the smoothing constant such as 0.05, 0.25, 0.50 and 0.75. Abbasi et al. and Khaliq et al. used these values of λ for constructing EWMA control chart under different non-normal distributions like Student's t, Gamma, Weibull etc. [46], [70]. We can use these factors directly to make the calculation easier. These W_1 and W_2 factors would be very helpful to construct the IMEWMA control chart for inverse *Maxwell* parameter easily.

It is to be mentioned that for some cases, especially smaller sample size, we may get negative lower limit and hence should be replaced by zero, as the proposed chart is to monitor scale parameter σ (cf. Table 5.5).

The above-mentioned limits given in (5.4) are called time varying limits of the IMEWMA charts. From Table 5.2, 5.3, 5.4 and 5.5 we notice that as the time i increases these limits converge to the constant limits for both known and unknown cases which are given as

$$LCL = \sigma_0^2\left[1 - L\sqrt{\frac{2}{3n}\times\frac{\lambda}{2-\lambda}}\right],$$
$$CL = \sigma_0^2,$$
$$UCL = \sigma_0^2\left[1 + L\sqrt{\frac{2}{3n}\times\frac{\lambda}{2-\lambda}}\right] \text{ and}$$
$$LCL = \bar{V}_{IM}\left[1 - L\sqrt{\frac{2}{3n}\times\frac{\lambda}{2-\lambda}}\right],$$
$$CL = \bar{V}_{IM}, \tag{5.5}$$
$$UCL = \bar{V}_{IM}\left[1 + L\sqrt{\frac{2}{3n}\times\frac{\lambda}{2-\lambda}}\right] \text{respectively.}$$

Hence, the factor $\left(1-(1-\lambda)^{2i}\right)$ in (5.4) will become 1 when the number of samples is large and ultimately the time variant limits at each sample point is utilized. Now, for monitoring an inverse *Maxwell* process the hypothesis are defined as

$H_0: \sigma^2 = \sigma_0^2$; or, $\delta = 1$, i.e. No shift occurs in the process.

$H_1: \sigma^2 = \sigma_1^2 = \delta\sigma_0^2$; or, $\delta \neq 1$, i.e. Shift occurs in the process.

Here, δ indicates the variation in the process.

5.2 Performance Evaluation of the IMEWMA control chart

The statistical performance of the IMEWMA control chart is evaluated in terms of the run length (RL) properties. Run length is the number in-control process before a signal is detected. There are several RL properties that are used by the researchers for measuring the performance of the control charts. In this study, we employed a Monte Carlo simulation method for the simulation. A code in R language which is a free software used for statistical graphics and computing has been developed to evaluate the run lengths [71].

By using estimated run lengths, we will estimate some properties that are used to evaluate our IMEWMA Control Chart. The description of RL properties is provided below.

Average Run Length (ARL): It is the most popular RL properties to investigate the performance of the control chart for the specific shifts. It indicates the average number of samples are required to get an out of control signal. The smaller ARL values is desired. The less the value is the more the chart is better. We can define this as

$$ARL = \frac{\sum_{i=1}^{m} RL_i}{m}$$

RL distribution of the of the inverse *Maxwell* distribution is positively skewed. So ARL is not sufficient to evaluate the suitability of the proposed chart. For this we also use the median run length and the standard deviation of the run length. The median of the RL is known as MRL and the standard deviation of the RL is called SDRL.

There are several performance tools are also available to examine the overall performance of the control chart that includes extra quadratic loss (EQL), relative average run length (RARL) and performance comparison index (PCI). The chart having smaller EQL, RARL and PCI values is considered to detect the shift more quickly than the others chart. The description of these tools is given as

Table 5.6: ARL, SDRL and MRL of IMEWMA chart for different n with $\lambda = 0.75$ at $ARL_0 \cong 370$.

	Sample size (n)								
	3			6			9		
δ	ARL	$SDRL$	MRL	ARL	$SDRL$	MRL	ARL	$SDRL$	MRL
1.00	373.11	372.52	258	373.31	373.83	258	371.36	371.44	260
1.05	235.75	235.43	163	191.73	191.38	133	174.63	176.82	119
1.10	150.03	150.20	105	109.05	107.59	77	91.96	90.74	65
1.15	99.91	98.95	70	67.65	67.66	47	51.08	51.88	35
1.20	70.22	69.81	49	43.59	42.51	30	31.50	31.47	22
1.25	50.66	50.19	36	28.88	29.04	20	20.40	20.16	14
1.35	29.49	28.54	21	15.39	15.38	11	10.00	9.67	7
1.50	15.49	15.14	11	7.45	7.16	5	4.71	4.52	3
1.75	7.23	6.85	5	3.24	2.95	2	2.05	1.62	1
2.00	4.21	3.86	3	1.94	1.50	1	1.36	0.80	1

Extra quadratic loss (EQL): The weighted average ARL over the entire shift domain ($\delta_{min} < \delta < \delta_{\max}$) using the square of shift as the weight is known as EQL. Mathematically it is defined as

$$EQL = \frac{1}{\delta_{max} - \delta_{min}} \int_{\delta_{min}}^{\delta_{max}} \delta^2 ARL(\delta) d\delta$$

where $ARL(\delta)$ is the ARL of a particular chart at shift δ and δ_{min} and δ_{max} are the minimum and maximum values of the shift.

Table 5.7: ARL, SDRL and MRL of IMEWMA chart for different n with $\lambda = 0.50$ at $ARL_0 \cong 370$.

Sample size (n)									
	3			6			9		
δ	ARL	$SDRL$	MRL	ARL	$SDRL$	MRL	ARL	$SDRL$	MRL
1.00	371.39	374.39	260	374.12	375.81	259	370.25	369.92	256
1.05	211.92	212.67	148	175.39	174.47	122	148.46	149.09	103
1.10	127.43	126.57	89	88.64	89.81	61	69.49	69.48	48
1.15	81.59	82.48	57	50.74	50.15	35	35.78	35.79	25
1.20	55.42	56.33	38	30.65	31.14	21	20.53	21.14	14
1.25	38.10	38.39	26	20.08	20.56	14	12.97	13.37	9
1.35	21.28	21.68	14	9.81	10.00	7	5.80	6.17	4
1.50	10.38	10.72	7	4.26	4.52	2	2.40	2.54	1
1.75	4.43	4.78	3	1.69	1.61	1	1.13	0.58	1
2.00	2.34	2.39	1	1.15	0.53	1	1.00	0.10	1

Relative average run length (RARL): The ratios average between the ARL of a particular chart ($ARL(\delta)$) with the benchmark chart ($ARL_{benchmark}(\delta)$) is called RARL. Mathematically RARL is given as

$$RARL = \frac{1}{\delta_{max} - \delta_{min}} \int_{\delta_{min}}^{\delta_{max}} \frac{ARL(\delta)}{ARL_{benchmark}(\delta)} d\delta$$

The chart for which the EQL is minimum is called the benchmark chart and for which the RARL is equal to one and for the all others competing charts RARL is greater than one.

Performance comparison index (PCI): The ratio of the EQL of a chart and the EQL of the best chart is known as PCI. Mathematically it can be derived as

$$PCI = \frac{EQL}{EQL_{best\ chart}}.$$

For the best chart PCI=1 and for the remaining charts $PCI > 1$.

The values of the average, standard deviation and median of the run length for different sample size and the values of the smoothing constant is given in the following tables.

Table 5.8: ARL, SDRL and MRL of IMEWMA chart for different n with $\lambda = 0.25$ at $ARL_0 \cong 370$.

	Sample size (n)								
	3			6			9		
δ	ARL	$SDRL$	MRL	ARL	$SDRL$	MRL	ARL	$SDRL$	MRL
1.00	374.63	374.24	262	373.90	371.92	262	372.05	364.90	262
1.05	181.65	184.53	126	141.18	143.77	98	121.17	124.81	82
1.10	94.33	96.42	65	61.70	64.61	42	43.87	48.36	29
1.15	54.24	57.45	37	28.94	33.59	18	18.22	22.33	10
1.20	33.88	36.99	22	14.63	18.22	8	7.83	11.48	2
1.25	21.48	25.18	13	7.83	11.27	2	3.41	5.80	1
1.35	8.99	12.14	3	2.19	3.73	1	1.13	1.01	1
1.50	2.60	4.36	1	1.00	0.19	1	1.00	0.00	1
1.75	1.00	0.25	1	1.00	0.00	1	1.00	0.00	1
2.00	1.00	0.00	1	1.00	0.00	1	1.00	0.00	1

In Table 5.6, we consider in-control situation and different out of control situations, take sample sizes 3, 6, 9 and the smoothing constant value is 0.75. We see that when the process is in control (δ =1) then the ARL is approximately equal to ARL_0 for all the considered sample sizes. For 20%, 50% and 75% (i.e. δ =1.2, 1.5 and 1.75) increment of shifts the average run lengths are approximately 70.22, 15.49 and 7.23 when the sample size is 3. It means that the ARL decreases as the shift increases for sample size 3. For the remaining sample sizes i.e. 6 and 9, the ARL follows same pattern as sample size 3. After 35% increment of shift the ARL reduce to 29.49, 15.39 and 10.00 from 370 for sample size 3, 6 and 9 respectively. It reviles that for $\delta = 1.35$, the ARL decreases as the sample size

increases. From Table 5.6, we see that for all other remaining increment of shifts the ARL diminishes for the enhancement of sample sizes like as 35% increment of shift.

In Table 5.6, the MRL and SDRL are also diminished for increment of shifts and sample sizes. Not only Table 5.6 but also Tables 5.7 and 5.8 in which we consider $\lambda = 0.5$ and 0.25 respectively exhibit the similar types of behavior in case of all types of run length properties. Into the above presented tables for sample size 9, the ARL values are 20.40, 12.97 and 3.41 at $\delta = 1.25$ and $\lambda = 0.75, 0.50$ and 0.25 respectively. It indicates that we obtained the smallest ARL at $\lambda = 0.25$. By the similar way the small values of SDRL and MRL can be achieved.

We also calculate the values of EQL, RARL and PCI for our designed IMEWMA control chart for sample size 6 at several values of λ. The values of these overall performance measurement tools are provided into Table 5.11. The RARL values of the proposed IMEWMA chart are 4.14, 2.52 and 1.00 for $\lambda = 0.75, 0.50$ and 0.25 respectively. So, it reduces as the smoothing constant decreases. Similarly, EQL and PCI are also reduced as λ decreases.

Based on the result presented in Tables 5.6-5.8 and 5.11, the main findings of our proposed chart is that IMEWMA chart is efficient at identifying small and moderate variations. A significant gain in performance of the proposed chart is achievable when smaller values of λ are used.

5.3 Simulation Study

We simulate data from inverse *Maxwell* distribution and confirmed that the generated data follows the distribution by using Kolmogorov-Smirnov (K-S) test. Interested readers are referred to Klugman et.al [70] for details of this procedure. In our case, we consider $\sigma_0 = 0.02$ and generate 120 sample observations by adopting K-S test, we failed to reject the null hypothesis that the data follow inverse *Maxwell* distribution.

Here, for the graphical representation of the IMEWMA control chart in case of the simulated data we consider the design parameters as $n = 6$, $\lambda = 0.25$ and $ARL_0 = 370$. To check the performance of the chart for detecting the process variations when it is out of control, we have considered a shift in the process scale parameter. We increased the scale parameter by 25% (i.e. $\delta = 1.25$) and 30% (i.e. $\delta = 1.3$) after the 10^{th} sample and constructed the proposed IMEWMA with the existing V_{IM} control charts (cf. Figure 2 and

3). It is obvious that for 25 % increment, there is no signal for the V_{IM} control chart, while IMEWMA chart signals for 3 data points. Similarly, for 30 % increment ($\delta = 1.3$) we notice that all the points are within the control limits for the V_{IM} chart while 8 data points are placed outside the control limits for the IMEWMA chart (cf. Figure 3).

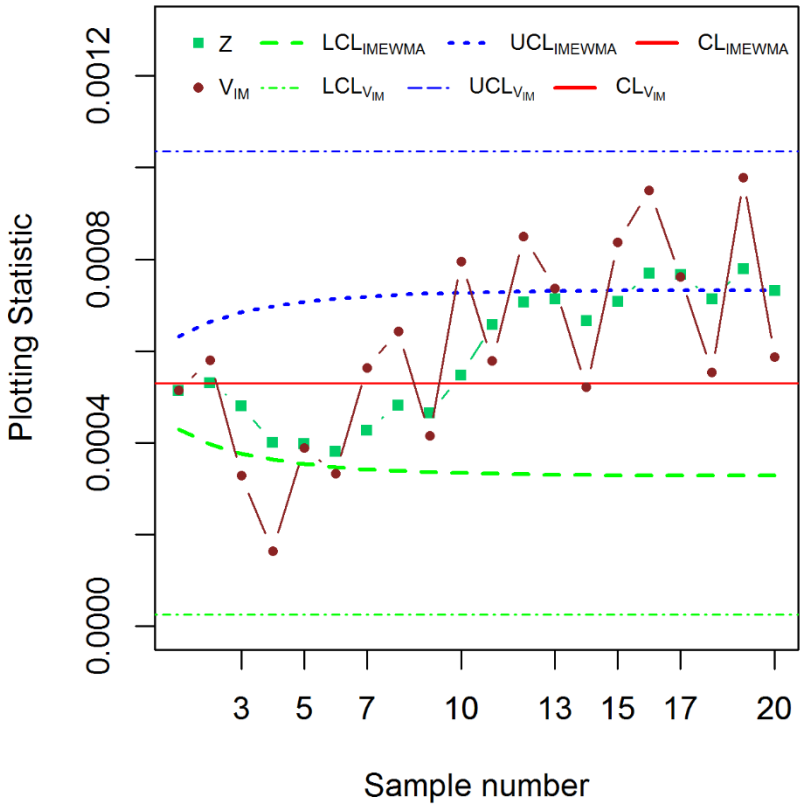

Figure 5.1: IMEWMA and V_{IM} charts for $\delta = 1.25$ and $\lambda = 0.25$.

In addition, we compare the proposed IMEWMA chart with Weibull distributed EWMA CEV control chart according to Zhang et al. [50] and Gan [41]. We consider the upper-sided control chart because while monitoring the *Maxwell* scale parameter, Hossain et al. reported that increase in variation is mostly disadvantage than decrease in variation [38]. To develop an upper-sided Weibull EWMA CEV control chart for monitoring an inverse *Maxwell* process, we set the process parameter as $\alpha_0 = 7.08$, $\beta_0 = 1.03$, $n = 6$, $\lambda = 0.25$, $ARL_0 = 370$, $K_u = 1.992$ and reflecting barrier (ω_0) equals to mean of the monitoring statistic which is 0.173. Considering 50% shift in the 10th sample, Figure 4 visualizes that the process is in control for Weibull EWMA CEV chart whereas the IMEWMA chart clearly identifies 9 out of control points after the 10th sample.

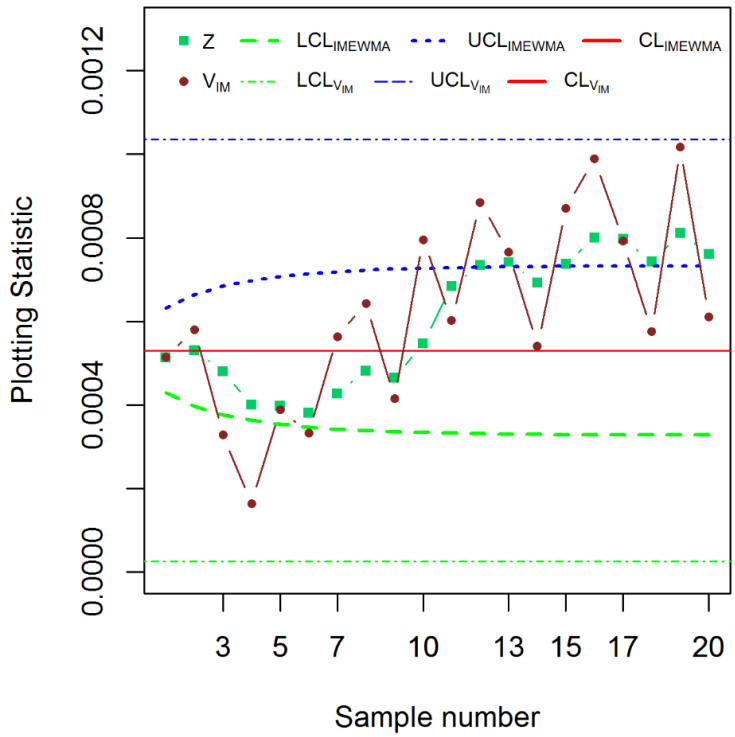

Figure 5.2: IMEWMA and V_{IM} chart for $\delta = 1.3$ and $\lambda = 0.25$.

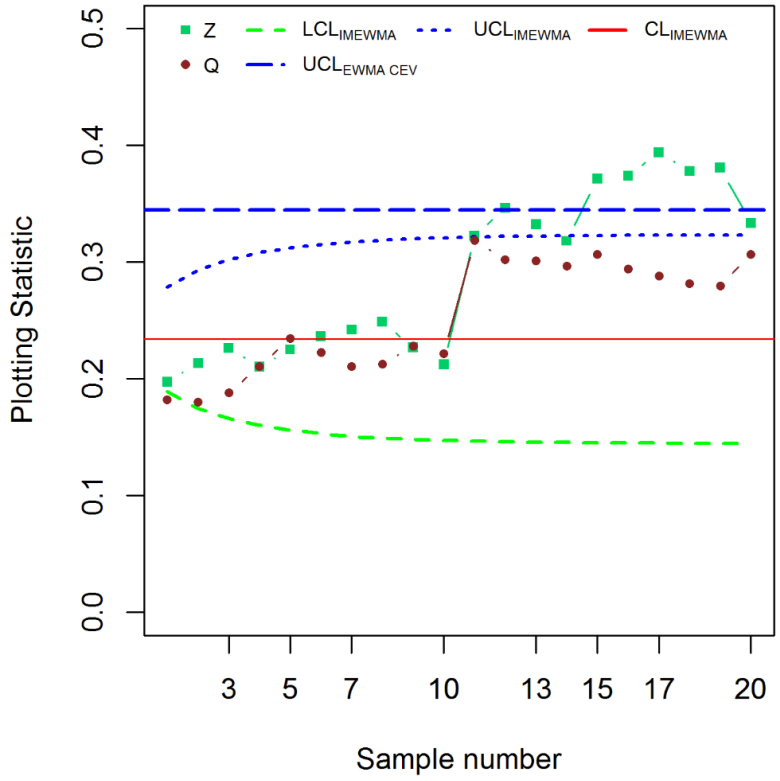

Figure 5.3: IMEWMA and upper-sided Weibull EWMA CEV chart for $\delta = 1.5$ and $\lambda = 0.25$.

It is evident that the proposed IMEWMA chart offers better detection ability as compared to V_{IM} and Weibull EWMA CEV charts for both small and moderate shifts. However, for larger shifts V_{IM} chart gets an edge over the new proposal and the considered Weibull EWMA CEV control chart is unsuitable to monitor an inverse *Maxwell* process.

5.4 Comparative studies

In this section, we provide a detailed comparison of the IMEWMA control chart with the V_{IM} chart along with IMCUSUM chart (which are the Shewhart and CUSUM type control chart for the inverse *Maxwell* distribution [22]). The performance of these control chart is compared in terms of ARL, MRL, EQL, RARL and PCI. In Table 5.11, the values of the overall performance tools (EQL, RARL and PCI) for both charts are given and their ARL and MRL values are also provided in Table 5.9 and 5.10. We also use the graphical representation to visualize the run length behavior of these two charts.

From Table 5.9, we see that the ARL of IMEWMA chart is less than the ARL of the $\mathrm{V_{IM}}$ chart. That means the ability of detecting shift of the IMEWMA chart is higher than that of $\mathrm{V_{IM}}$ chart. The ARL values are gradually decreasing as the shift increases. We also conclude that the IMEWMA chart works better than the $\mathrm{V_{IM}}$ chart as the smoothing constant decreases, e.g. ARL becomes the smallest when $\lambda = 0.25$. The median run length also exhibits the similar behavior. We have also produced Figures 5.3 and 5.4 in support of the results that we state about the behavior of ARL and MRL based on Tables 5.9 and 5.10.

Table 5.9: ARL for IMEWMA, IMCUSUM and V_{IM} chart at $\mathrm{ARL_0} \cong 370$ with $n = 6$.

	δ	1.00	1.05	1.10	1.15	1.20	1.25	1.35	1.50	1.75	2.00
V_{IM}		373.32	287.01	202.79	130.73	88.22	61.22	31.54	14.58	5.86	3.39
IMCUSUM		370.32	116.73	48.85	37.55	20.08	16.88	14.24	7.45	5.24	4.94
IMEWMA	$\lambda = 0.75$	373.31	191.73	109.05	67.65	43.59	28.88	15.39	7.45	3.24	1.94
	$\lambda = 0.50$	374.12	175.39	88.64	50.74	30.65	20.08	9.81	4.26	1.69	1.15
	$\lambda = 0.25$	373.90	141.18	61.70	28.94	14.63	7.43	2.19	1.00	1.00	1.00

This comparative analysis of ARL and MRL also evince that the IMCUSUM chart perform better for small variations comparative to IMEWMA chart, especially when the smoothing constant, λ is moderate. But the superiority of this CUSUM type control chart diminishes as the variations increased than the EWMA type control chart for any value of the smoothing constant.

Table 5.10: MRL for IMEWMA, IMCUSUM and V_{IM} chart at $ARL_0 \cong 370$ with $n = 6$.

	δ	1.00	1.05	1.10	1.15	1.20	1.25	1.35	1.50	1.75	2.00
V_{IM}		258	197	137.5	90	60	43	22	10	4	2
IMCUSUM		280	118	67	41	27	9	8	6	2	2
IMEWMA	$\lambda = 0.75$	258	133	77	47	30	20	11	5	2	1
	$\lambda = 0.50$	259	122	61	35	21	14	7	2	1	1
	$\lambda = 0.25$	262	98	42	18	8	2	1	1	1	1

Table 5.11: EQL, RARL and PCI of RL of IMEWMA, IMCUSUM and V_{IM} chart for different λ at $ARL_0 \cong 370$.

	V_{IM}	IMCUSUM	IMEWMA		
			λ		
			0.75	0.50	0.25
EQL	79.52	37.63	47.80	38.32	26.96
RARL	8.00	4.14	4.14	2.52	1.00
PCI	2.95	1.40	1.77	1.42	1.00

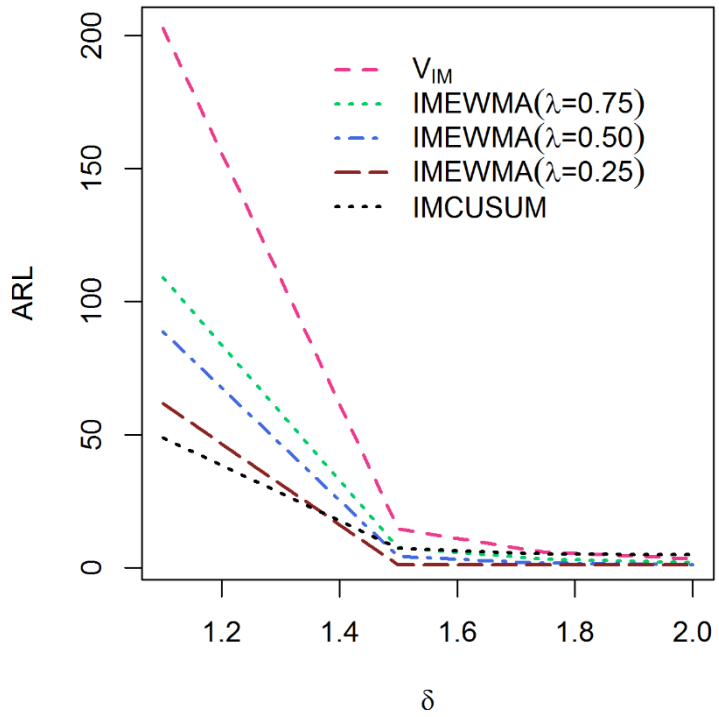

Figure 5.4: ARL curves for IMEWMA, IMCUSUM and V_{IM} chart at $n = 6$.

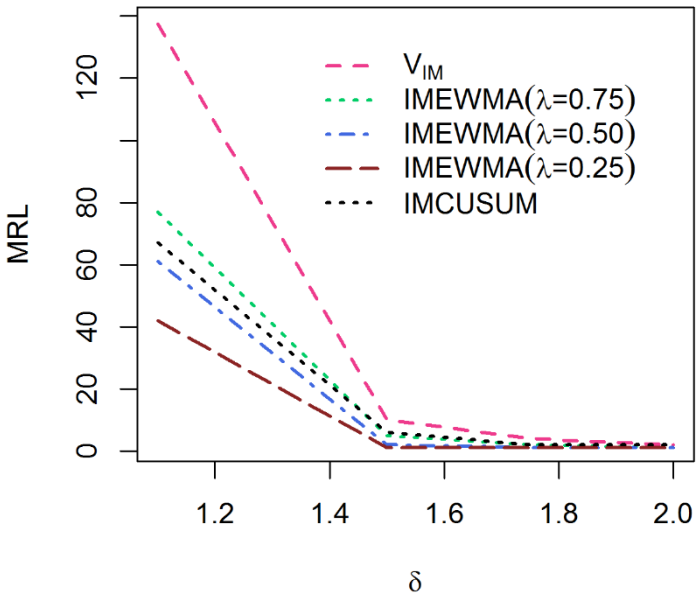

Figure 5.5: MRL curves for IMEWMA, IMCUSUM and V_{IM} chart at $n = 6$.

Moreover, we have also analyzed the performance of the competing charts using EQL, RARL and PCI. For an optimum chart, we expect these measures to be low. From Table 5.11, we see that all these overall performance measures of the IMEWMA chart are less than the V_{IM} chart. It is also evident from this table that, the overall performance measure values are equal to IMEWMA control chart when λ is close to 0.75 which means for small and moderate values of the smoothing constant our proposed IMEWMA chart is outperform than the existing chart. In our comparison we have considered $n = 6$ but for all other sample size it holds the similar behavior. So, we conclude that the proposed IMEWMA chart of this chapter works better than the V_{IM} chart as well as IMCUSUM chart to detect small and moderate shifts.

5.5 Real-life example

For illustrating the performance of our proposed IMEWMA chart, the real dataset was collected from [69]. Brake pad is a key component of vehicles breaking system. The lifetime of cars' brake pad is the distance covered by the vehicles when the brake pads are installed [53]. This dataset contains 98 vehicles brake pads lifetime. Under the null hypothesis that the dataset follows inverse *Maxwell* distribution, the K-S test statistic value is 0.105 where at 1% level of significance the critical value is 0.144 and the p-value is

0.452. Clearly the calculated value is less than the tabulated value of K-S test statistic and p-value is larger than the level of significance, so we cannot reject the null hypothesis that the data follows inverse *Maxwell* distribution. Hence, we can use this dataset for the construction of our proposed chart. After truncation the data cover 72 samples, each of subgroup size six.

Now on the basis of Section 5.1, for cars' dataset, the estimated value of the MLE $\bar{V}_{IM} = 8.810865 \times 10^{-5}$. From Table 5.3 for fixed in control average run length (ARL_0) value, $\lambda = 0.25$ and $n = 6$, we have 12 pairs of factors that are multiplied by the estimated MLE of the process scale parameter to get the time varying control limits. Now the graphical display of the IMEWMA chart based on these values are given in Figure 7.

From [71], we know that there are several criterions for detecting the lack of control such as a point outside the control limits, a run of seven points or more, a run of points beyond some secondary limits, the points are too close to the central line, presence of trends and presence of cycles. None of the above criteria are present in Figure 7. So, we can say that the process is in control.

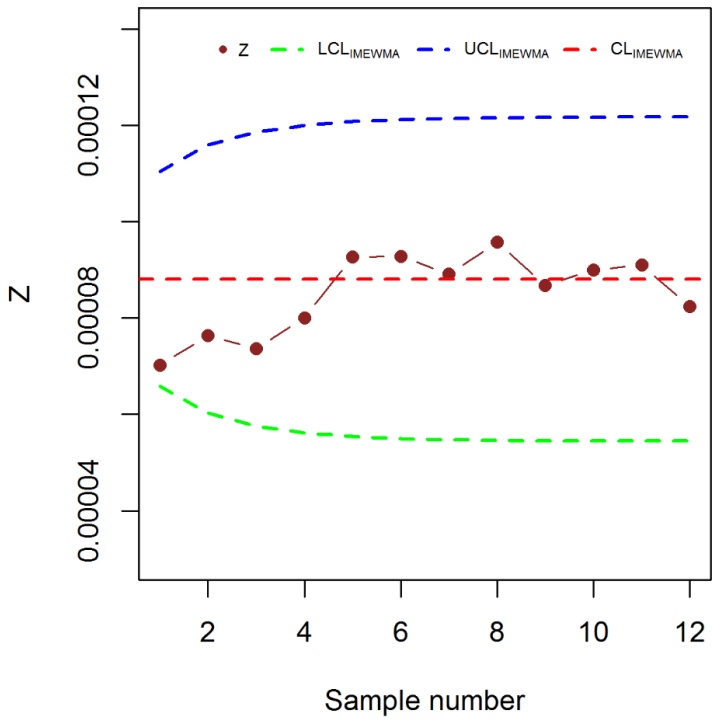

Figure 5.6: IMEWMA chart for cars' brake pad lifetime at $\delta = 1$.

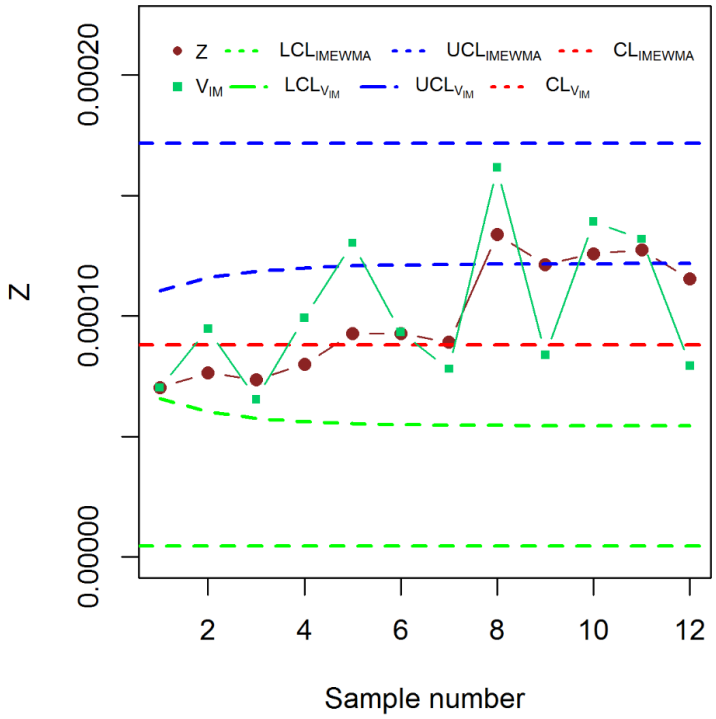

Figure 5.7: IMEWMA and V_{IM} chart for cars' brake pad lifetime at $\delta = 1.40$ (after 7th sample).

Some real situation where lifetime of brake pads is low or high for some special reason like different manufacture of vehicle, road conditions etc. By considering these situations for testing the sensitivity and comparison of our proposed chart to shifts in process scale parameter with V_{IM} chart. We learn that our proposed chart is more sensitive than the V_{IM} chart on the basis of run length properties and simulated data. For this to check whether our proposed chart is capable or not to detect the small and moderate deviation of shifts, in case of each of the last 5 data points we consider $\delta = 1.40$ for IMEWMA chart. That means we ponder 40% increment of variations. Hence, among the 12 data points, the first 7 data points are in control, whereas the last 5 data points are out of control. In Figure 8 we visualize the V_{IM} and IMEWMA chart and take $\delta = 1.40$ after 7^{th} sample respectively. From Figure 8, we see that although 40% increment of shifts the process is still in control in case of V_{IM} chart and on the basis of IMEWMA chart that easily detect the shifts and make the process out of control because among the 5 points, 4 points are outside the control limits. Hence from our cars' brake pads lifetime we can conclude that our proposed IMEWMA control chart can detect small and moderate shifts and its shift detecting ability is further better than the V_{IM} chart.

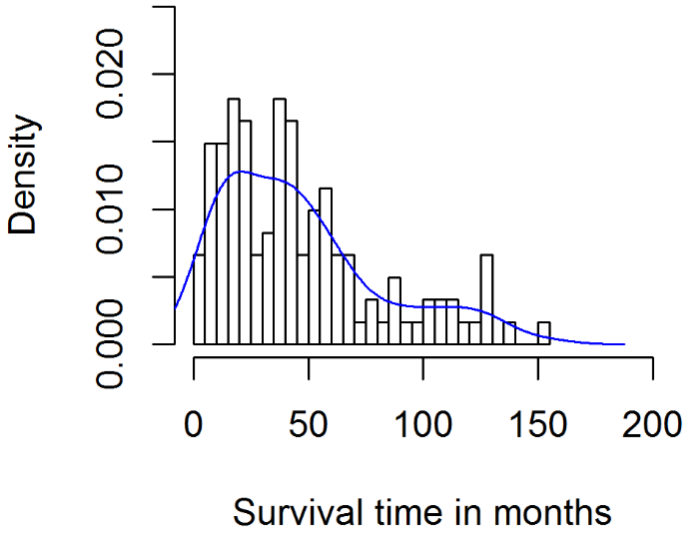

Figure 5.8: The distribution of survival time for breast cancer patients.

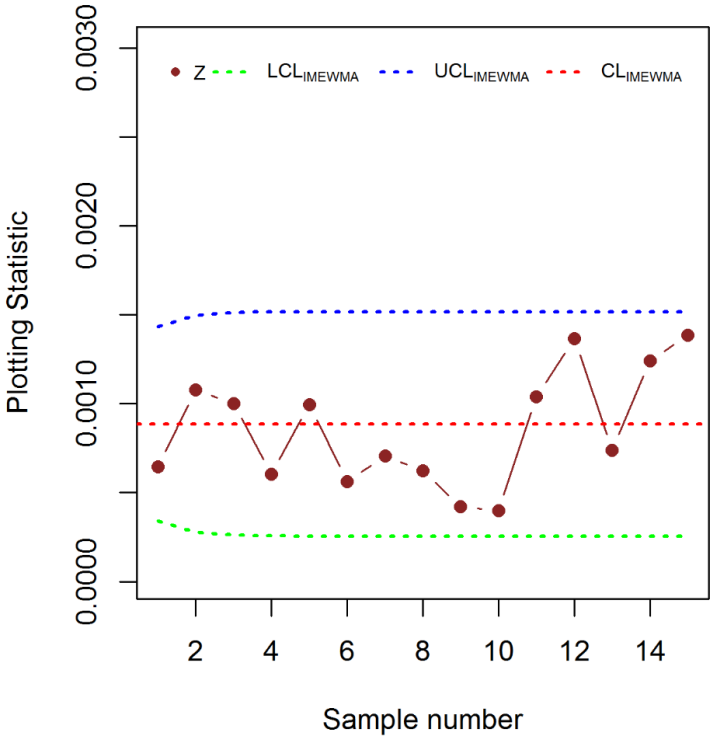

Figure 5.9: IMEWMA chart for survival time for breast cancer patients at $\delta = 1$.

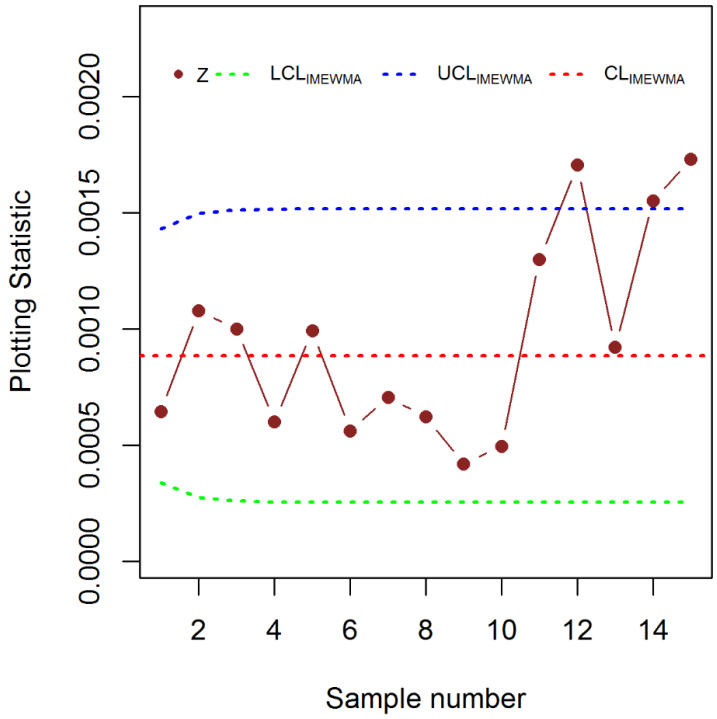

Figure 5.10: IMEWMA chart for survival time for breast cancer patients at $\delta = 1.25$ (after 9th sample).

To popularize the inverse *Maxwell* distribution, we have considered another real-life example. From literature, we have learnt that inverse *Maxwell* distribution deals with more skewed filed than the *Maxwell* and other popular distribution. The abnormal growth of cells beyond their usual boundaries that invades adjoining parts of the body and spread to other organs is characterized by a generic term Cancer. The world health organization (WHO) declared breast cancer as the most frequent cancer among women which early impacts more than 2 million women and causes the greatest number of cancer related deaths [54]. This depicts the necessity for monitoring the survival time of breast cancer that helps us to provide actual treatment among the patients. The distribution of survival time for breast cancer patients is skewed (cf. Figure 9). This drive us to use the inverse *Maxwell* distributed IMEWMA control chart for monitoring the survival time for breast cancer patients. Moreover we also failed to reject the null hypothesis that the survival time data set provided in [69] follows inverse *Maxwell* distribution with the K-S test statistic value 0.138 where at 5% level of significance the critical value is 0.178.

To construct the IMEWMA control chart for breast cancer dataset, we randomly choose 15 subgroups of size 5 from 121 data points. The IMEWMA chart contains all the 15 plotting

statistic points into its limit bands which indicates that the chart clearly identifies the process when it is in control (cf. Figure 10). For ensuring its ability to detect variations, we intentionally increase the shift by 25% after the first 9 samples and our proposed chart detect 3 out of control samples among the last 6 samples (cf. Figure 11). Finally, we strongly suggest implying IMEWMA control chart for monitoring the skewed process like survival lifetimes.

5.6 Summary of the IMEWMA control chart

In this chapter, we designed a control chart named IMEWMA chart for monitoring a process under inverse *Maxwell* distribution. The proposed chart is based on the MLE of scale parameter of the inverse *Maxwell* distribution. The performance of the IMEWMA chart is investigated in terms of several run length properties like ARL, SDRL and MRL. We have also evaluated the proposed chart by using some overall performance measuring tools such as EQL, RARL and PCI. Based on the values of these measures it has been observed that the best performance of the IMEWMA chart is obtained at small to moderate levels of the smoothing parameter, and it keeps improving with the increase in sample size. The comparative analysis advocates that for small smoothing constant values, our proposed chart is more effective than the existing V_{IM} chart and IMCUSUM chart for small and moderate shifts. Moreover, we have carried out a simulation study to exhibit the construction procedure of our prosed chart under inverse *Maxwell* distribution. We have also considered a real-life scenario and implicate our designed IMEWMA chart to monitor the process of lifetimes of cars brake pads. In the next chapter, we will introduce another control chart namely CIM-VEWMA.

CHAPTER SIX

COMBIINED IM-VEWMA CONTROL CHART

Combined control charts are extensively used to identify small and moderate assignable cause variations in industrial process monitoring. As a member of memory type control chart, Lucas et al. the proposed the design of Combined Shewhart-EWMA (CSEWMA) [53]. This chart is based on the normality assumption for this we introduce a new CSEWMA type chart in case of non-normal distribution. In our case we consider inverse *Maxwell* distribution as a candidate of non-normal distribution and we named our developed chart as CIM-VEWMA control chart. In this chapter, we describe the design procedure of the CIM-VEWMA control chart along with its numerical performance analysis and application.

6.1 General Structure of Combined IM-VEWMA Chart

Let the outcome of a production process of interest is characterized by a random variable R that follows inverse *Maxwell* distribution with a single scale parameter $\delta\sigma_0$, where σ_0 is known and δ refers to the amount of shifts. If $\delta = 1$, then the production process is in control, otherwise the process contains shifts. We also consider that the samples obtained at time $i = 1, 2, 3 \ldots \ldots$ are mutually independent. The addition of V_{IM} control limits to the IMEWMA control chart is introduced as combined IM-VEWMA control chart. The proposed CIM-VEWMA charts consists of two plotting statistics, one for the Shewhart type control chart and the other for memory type control chart. In our case, the Shewhart and memory type control charts are the V_{IM} and IMEWMA charts respectively. The proposed chart has three parameters named as lower control limit (LCL), center line (CL) and upper control limit (UCL). It has two LCL, named as LCL_S and LCL_M and they stand for V_{IM} and IMEWMA charts respectively. Similarly, the upper control limits are denoted by UCL_S and UCL_M.

To monitor an inverse *Maxwell* process, we assume a random variable V_{IM}, where $V_{IM} = \hat{\sigma}^2$ distributed as gamma distribution with mean σ^2 and variance $\frac{2\sigma^4}{3n}$. The V_{IM} chart uses the present facts based on the statistic V_{IM_i} for monitoring the process, while the IMEWMA control chart use the following statistic

$$Z_i = \lambda V_{IM_i} + (1 - \lambda) Z_{i-1}, \tag{6.1}$$

where Z_{i-1} and V_{IM_i} are the previous and present facts, respectively and λ is a smoothing constant with $0 < \lambda \leq 1$. The mean and variance of W_i is σ^2 and $\frac{2\sigma^4}{3n}\left(\frac{\lambda}{2-\lambda}\right)$ respectively.

The Combined IM-VEWMA control chart detect the out of control signals when either the statistic V_{IM_i} falls outside the V_{IM} control chart limits

$$LCL_S = \left[1 - L\sqrt{\frac{2}{3n}}\right]\sigma^2 \text{ and } UCL_S = \left[1 + L\sqrt{\frac{2}{3n}}\right]\sigma^2, \tag{6.2}$$

or the statistic W_i falls outside the IMEWMA control limits

$$LCL_M = \left[1 - L\sqrt{\frac{2\lambda}{3n(2-\lambda)}}\right]\sigma^2 \text{ and } UCL_M = \left[1 + L\sqrt{\frac{2\lambda}{3n(2-\lambda)}}\right]\sigma^2. \tag{6.3}$$

The center line is same for the both $V_{IM}$and IMEWMA control charts i.e. $CL_S = CL_M = \sigma^2$. So, for our proposed chart $CL = \sigma^2$. If we know the target value of the scale parameter, σ then all σ^2 of equation (6.2) and (6.3) are replaced by σ_0^2 otherwise replaced by the estimated value from the preliminary in-control information i.e. $\bar{V}_{IM}$. The detailed design procedure of the individual V_{IM} and IMEWMA control charts are provided in Arafat et al. [22] and Chapter five respectively.

6.2 Performance analysis

To access the statistical performance of our proposed control chart, we studied several run length properties named as average run length (ARL), standard deviation of run length (SDRL) and median of run length (MRL). There are three ways to estimate the run length of control chart, the integral equation method, the Markov chain approach and Monte Carlo simulation method [66]. We used Monte Carlo simulation method and assume that an in-control process follows an inverse *Maxwell* distribution with $\sigma_0 = 0.2$. In R 3.3.4 a simulation study has been conducted to estimate the run lengths by the following steps:

Step 1: Random subgroups of size n are generated from inverse *Maxwell* distribution.

Step 2: Determine the design parameters for appropriate constant λ and sample size n.

Step 3: Construct the control limits using equation (6.2) for the constant limits and equation (6.3) for the time-varying limits.

Step 4: Use the generated samples to estimate the plotting statistics V_{IM_i} and Z_i.

Step 5: Compare the plotting statistics with the control limits.

Step 6: The number of samples, at which V_{IM_i} falls outside of LCL_S & UCL_S, is observed and consider it as run length of V_{IM} chart.

Step 7: Again, the number of samples, at which Z_i falls outside of LCL_M & UCL_M, is defined as the run length of IMEWMA chart.

Step 8: Carried out 10,000 iterations and the minimum value of Steps 6 and 7 is defined as the run length of the proposed CIM-VEWMA chart. Symbolically denoted by,

$$RL_{CIM-VEWMA} = minimum\ (RL_{V_{IM}}, RL_{IMEWMA}).$$

Table 6.1: ARL values of the Combined IM-VEWMA control chart at ARL0 ≅370.

Smoothing constant (λ)									
	0.75			0.50			0.25		
δ \ n	3	6	9	3	6	9	3	6	9
1.00	370.23	369.84	372.54	370.62	373.61	370.67	369.41	371.89	370.28
1.05	198.26	184.64	166.37	196.27	160.08	140.92	170.51	130.26	80.19
1.10	130.27	100.76	80.24	118.59	80.61	60.13	88.67	50.37	30.38
1.15	81.68	55.19	46.66	72.91	41.49	30.46	48.39	18.94	11.67
1.20	53.67	38.97	24.73	48.11	22.54	14.33	24.44	9.37	2.36
1.25	37.93	22.49	14.86	30.98	13.73	7.93	14.89	5.28	1.87
1.35	18.60	14.63	8.44	14.82	6.36	3.74	6.27	1.86	1.00
1.50	9.37	5.45	3.08	7.63	2.58	1.86	1.26	1.12	1.00
1.75	4.93	2.97	1.85	2.86	1.19	1.08	1.11	1.06	1.00
2.00	2.58	1.38	1.04	1.57	1.00	1.00	1.06	1.00	1.00

The ARL is enumerated at a specific shift point because of this Wu et al. have raised concern about the suitability of ARL for measuring performance of control charts [67]. Consequently, we further use some overall performance measuring tools like as extra quadratic loss (EQL), relative average run length (RARL) and performance comparison index (PCI). Below is a brief description of required measures.

$ARL = E(RL_{CIM-VEWMA}), MRL = Median\ (RL_{CIM-VEWMA}),$

$SDRL = \sqrt{E(RL_{CIM-VEWMA})^2 - \{E(RL_{CIM-VEWMA})\}^2},$

$EQL = \frac{1}{\delta_{max}-\delta_{min}} \int_{\delta_{min}}^{\delta_{max}} \delta^2 ARL(\delta) d\delta$,

$RARL = \frac{1}{\delta_{max}-\delta_{min}} \int_{\delta_{min}}^{\delta_{max}} \frac{ARL(\delta)}{ARL_{benchmark}(\delta)} d\delta$ and $PCI = \frac{EQL}{EQL_{benchmark}}$,

where E stands for the expected value, $ARL(\delta)$ is the ARL of a particular chart at shift δ, δ_{min} and δ_{max} are the minimum and maximum values of the shift, $ARL_{benchmark}(\delta)$ and $EQL_{benchmark}$ are the ARL and EQL of the best chart at δ respectively. The smaller values for these measures are expected. For the benchmark chart, we consider the value of RARL and PCI equal to one and for other charts it is more than one [68].

We use subgroup sizes of $n = 3, 6, 9$ and set in-control ARL_0 value for the control chart at 500. We also consider the smoothing constant values $\lambda = 0.25, 0.50$ and 0.75. The performance of the proposed chart is investigated for different shift sizes say $\delta = 1.00, 1.05, 1.10, 1.15, 1.20, 1.25, 1.35, 1.50, 1.75$ and 2.00. The computed ARL, SDRL and MRL values are displayed in Tables 6.1-6.3. Table 6.4 covers the overall measures including EQL, RARL and PCI under different values of λ.

Table 6.2: SDRL values of the Combined IM-VEWMA control chart at ARL0 ≅370.

Smoothing constant (λ)									
	0.75			0.50			0.25		
δ \ n	3	6	9	3	6	9	3	6	9
1.00	371.20	372.36	371.14	371.22	372.55	370.47	371.69	370.07	372.77
1.05	196.99	183.19	166.78	198.36	160.74	136.49	172.69	129.89	80.85
1.10	131.28	99.47	81.38	117.48	78.67	58.67	90.53	50.88	31.47
1.15	79.38	54.26	47.87	71.24	39.67	29.69	47.43	19.04	11.96
1.20	54.69	40.64	23.67	49.69	22.16	14.89	24.99	9.93	1.67
1.25	37.67	23.59	14.41	31.09	14.49	6.88	15.03	4.92	0.87
1.35	17.89	14.08	8.09	13.87	5.98	3.69	4.89	2.91	0.56
1.50	10.14	5.97	4.17	7.89	2.41	1.04	0.99	0.87	0.44
1.75	4.69	2.87	1.46	1.58	0.59	0.46	0.34	0.24	0.24
2.00	2.14	1.18	0.84	0.73	0.33	0.27	0.22	0.14	0.10

The performance of our proposed CIM-VEWMA control chart based on different performance measures values that are presented in Table 6.1- 6.4 and Figure 6.1, advocate the following conclusions:

1. The average run length (ARL) is always smaller than ARL_0 (i.e. in-control ARL) for any choice of shift, δ and it also concludes that the proposed chart is truly proficient at detecting small, moderate and large shifts (cf. Table 6.1).

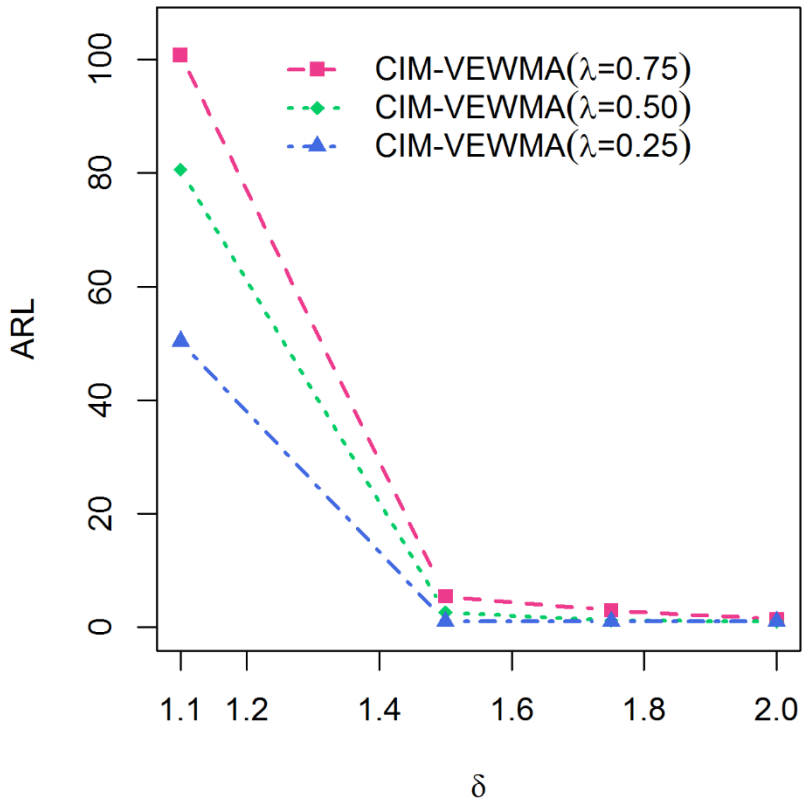

Figure 6.1: ARL curves of CIM-VEWMA control chart for $n = 6$ at λ=0.75,0.50 and 0.25.

2. When the process is in control, i.e.$\delta = 1$, there is no significant difference between the SDRL values and the corresponding ARL values for any sample size, n and smoothing constant, λ. For example: The ARL and SDRL values are 373.61 and 372.55 respectively at $n = 6$ and $\lambda = 0.50$, Similarly, when $n = 3$ and $\lambda = 0.25$, the ARL and SDRL values are 369.41 and 371.69 respectively (cf. Tables 6.1 and 6.2).
3. The ARL and SDRL values rapidly decrease as the shift increases in the process scale parameter. For example: At 10% increment of shift the ARL and SDRL are 130.27 and 131.28 respectively for $n = 3$ and $\lambda = 0.75$ and under same parameters at 50% increment of shift the ARL and SDRL become 9.37 and 10.14. From these values, we can also conclude that the ARL and SDRL are directly proportional to each other (cf. Tables 6.1 and 6.2).
4. In case of both in and out of control situations and for any combination of n and λ, the ARL values are greater than the MRL values. It indicates that the run length distribution of the CIM-VEWMA chart is positively skewed. For example: when $n =$

9, $\delta = 1.5$ and $\lambda = 0.50$, the ARL and MRL values are 1.86 and 1 respectively. Also, for $n = 3$, $\lambda = 0.75$ and $\delta = 2$, the ARL and MRL values are 2.58 and 2 correspondingly (cf. Tables 6.1 and 6.3).

Table 6.3: MRL values of the Combined IM-VEWMA control chart at ARL0 ≅370.

Smoothing constant (λ)									
	0.75			0.50			0.25		
δ \ n	3	6	9	3	6	9	3	6	9
1.00	260	258	262	256	258	263	261	262	259
1.05	158	130	100	140	111	96	120	94	74
1.10	96	70	59	84	55	43	56	38	16
1.15	64	42	31	51	33	21	32	11	7
1.20	40	25	14	33	17	6	17	5	3
1.25	30	14	10	22	11	3	9	3	1
1.35	16	8	5	10	5	2	2	2	1
1.50	5	3	2	5	2	1	1	1	1
1.75	4	1	1	2	1	1	1	1	1
2.00	2	1	1	1	1	1	1	1	1

5. Smaller values of λ makes the proposed chart more sensitive to small shifts but for detecting large shifts the effect of λ is not that worthy. It is observed in Figure 6.1.
6. Almost all the performance measures including ARL and MRL show that the proposed chart not only maintain the shift detecting ability of IMEWMA and V_{IM} chart for small and large shifts correspondingly but also received better moderate shifts handing ability (cf. Tables 6.1-6.3).
7. ARL values are diminished as the enhancement of sample size, n. For example: The ARL values for $\delta = 1.75$ and $\lambda = 0.50$ are 2.86, 1.19 and 1.08 when $n = 3, 6$ and 9 respectively (cf. Table 6.1). Almost the alike behavior is exhibited for SDRL and MRL (cf. Tables 6.2 and 6.3).
8. As the process goes out of control, i.e. $\delta > 1$, the proposed CIM-VEWMA chart offer better performance for small smoothing constant value. It is evident by different

measures such as ARL and other performance measures. For example: The ARL values are 37.93, 30.98 and 14.89 for $\lambda = 0.75, 0.50$ and 0.25 respectively at $\delta = 1.25$ and $n = 3$. For same sequence of λ values, 22, 11 and 3 are the values of MRL for $n = 6$. It is evident that both ARL and MRL are the smallest at $\lambda = 0.25$.

9. On the overall performance of the proposed chart in diagnosing both transient and persistent variations, we also suggest that the CIM-VEWMA chart substantially avails more proficiency as λ diminished. The supporting results provided in Table 6.4. For example: The RARL values are 1, 2.42 and 3.70 correspondingly for $\lambda = 0.25, 0.50$ and 0.75. Similarly, for same order of λ, the PCI values are 1, 1.40 and 1.78 respectively.

6.3 Comparisons of Control Charts

To examine the effectiveness of our proposed CIM-VEWMA control chart, we compare its' ARL performance with some of the existing chart suitable for detecting small, moderate and large variations in the process scale parameter when the underline distribution is inverse *Maxwell*. In this study, the control charts used for comparison including IMEWMA control chart and V_{IM} control chart as well as IMCUSUM chart. We also use several overall performance measures for better comparison that includes PCI, EQL and RARL. We consider subgroup size of $n = 6$, while the cases based on other sample sizes concludes the similar behavior. Using the in-control ARL of 370 and shift, $\delta = 1.10, 1.25, 1.50, 1.75$ and 2.00. All numerical values required for comparison are provided in Tables 6.4 and 6.5. Based on the shift classifying ability, the charts are arranged from left to right into the tables.

Proposed versus V_{IM} chart: V_{IM} control chart is a Shewhart type chart and this type of chart is the most popular choice among the researchers to monitor large shifts in the process. The proposed chat has not only smaller ARL values but also has smaller EQL, PCI and RARL values than V_{IM} chart for any choice of λ. For example: At 50% increment of shift the ARL values are 2.58 and 14.58 for the proposed and V_{IM} chart respectively and for $\lambda = 0.50$, RARL value of CIM-VEWMA is 2.42 whereas for V_{IM}, it is 8.55. Though the V_{IM} chart is popular for larger shift but here our proposed chart exhibits better ARL performance than V_{IM} chart in case of large shift. This means that the suggested chart can detect large shift faster than the V_{IM} chart. The proposed chart will earn more edge over the V_{IM} chart as the smoothing constant, λ decreases. The supporting results provide in Tables 6.4 and 6.5.

Proposed versus IMEWMA: As a candidate of memory type control chart, EWMA chart extensively applied to detect small and moderate shifts. IMEWMA is also used for the similar purpose under inverse *Maxwell* distribution. The overall and individual performance measures

values indicate the superiority of the proposed chart over the IMEWMA chart for small and large shifts. Because all these performance measures values of the IMEWMA chart are larger than the proposed chart. For example: The PCI and EQL values of the IMEWMA chart are 22.96 and 47.80 at $\lambda = 0.75$ whereas these are 24.1 and 43.36 for CIM-VEWMA. The efficiency is increased in case of the both charts for smaller values of λ. For 50% changes into λ, the ARL is changed by around 46% and 58% for the proposed chart and IMEWMA chart respectively (cf. Table 6.5). It indicates that the suggested CIM-VEWMA chart is less sensitive to λ compared to IMEWMA chart.

Table 6.4: Overall performance comparison among IMEWMA, CIM-VEWMA, IMCUSUM and VIM at ARL0 ≅370.

	CIM-VEWMA			IMEWMA			IMCUSUM	V_{IM}
λ	0.25	0.50	0.75	0.25	0.50	0.75		
EQL	24.31	32.54	43.36	26.96	38.32	47.80	37.63	79.52
RARL	1	2.42	3.70	1.09	2.73	4.40	4.70	8.55
PCI	1	1.40	1.78	1.11	1.58	1.97	1.55	3.27

Table 6.5: ARL comparison among IMEWMA, CIM-VEWMA, IMCUSUM and VIM when n=6 at ARL0 ≅370.

	CIM-VEWMA			IMEWMA			IMCUSUM	V_{IM}
δ \ λ	0.25	0.50	0.75	0.25	0.50	0.75		
1.10	50.37	80.61	100.76	61.70	88.64	109.05	48.85	202.79
1.25	5.28	13.73	22.49	7.43	20.08	28.88	16.88	61.22
1.50	1.12	2.58	5.45	1.00	4.26	7.45	7.45	14.58
1.75	1.06	1.19	2.97	1.00	1.69	3.24	5.24	5.86
2.00	1.00	1.00	1.38	1.00	1.15	1.94	4.94	3.39

Proposed versus IMCUSUM: The cumulative sum control chart is usually implemented to identify small shifts. For our considered inverse Maxwell distribution, we observe this similar properties. The proposed chart which is the combination of EWMA and Shewhart type control chart exhibits better performance than the IMCUSUM chart for detecting moderate and large shift but under small amount of variations the CUSUM type control chart is still superior. For example: At 10% increment of variations the average run length is 50.37 for CIM-VEWMA control chart at $\lambda = 0.25$ whereas the ARL is 48.85 for IMCUSUM chart. But for 50% increment the ARL is 1.12 and 7.45 for the comparative charts. Finally the overall

performance measures show the superiority of the proposed chart because 24.31 and 37.63 is the values of EQL for CIM-VEWMA and IMCUSUM chart respectively.

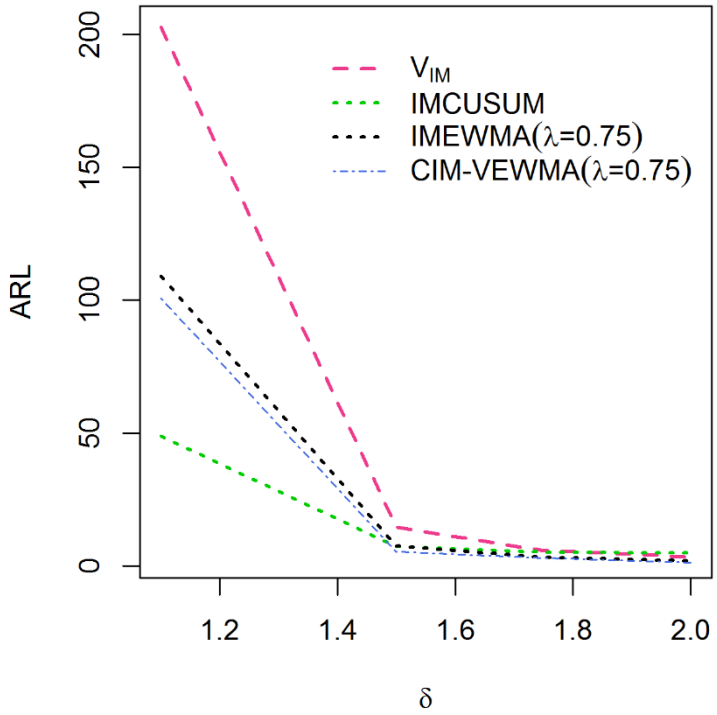

Figure 6.2: ARL curves for the proposed CIM-VEWMA at λ=0.75, IMEWMA and VIM chart.

To extract some hidden information from the above tables and visualize the superiority of our proposed CIM-VEWMA chart over others, we have provided some graphical presentations of ARL curves. In Figure 6.2, the proposed chart at $\lambda = 0.75$ is compared with V_{IM} chart and IMEWMA chart at $\lambda = 0.75$. The ARL curve of the proposed CIM-VEWMA is at the lower side for large and moderate shifts but it nearly overlaps with the ARL curve of $IMEWMA_{\lambda=0.25}$ for small shifts, which is evidence of similar performance just in case of small shifts of the proposed chart with $IMEWMA_{\lambda=0.25}$. Similarly, the proposed chart is superior to IMCUSUM chart for moderate and large shift. Figure 6.2 visualizes the outperforming behavior of the proposed chart compared to the others and indicates that for smaller values of the smoothing constant, the sensitivity of the CIM-VEWMA chart is boosted for detecting shifts, especially for moderate and large shifts.

6.4 Example of Application

To illustrate the application of our proposed chart, we consider a real dataset related to cars' brake pads lifetime. The data were collected from [69]. Summary of the implemented dataset is given below. Brake pad is a key component of car breaking system which converts the kinetic energy of the car to thermal energy by friction that slows and stops the wheel. It works with a very thin layer of material and generate semi-liquid friction that creates the actual

braking force [70]. Figure 5.4 visualizes the major components of vehicles breaking system including brakes pads. The amount of distance covered the vehicles while the brake pads are installed into the vehicles breaking system is defined as lifetime of cars' brake pad. The dataset contain 98 observations and lifetimes are provided in kilometers. To check whether the data follow inverse *Maxwell* distribution or not, we perform K-S test, under the null hypothesis that the dataset follow inverse *Maxwell* distribution. At 1% level of significance (i.e. $\alpha = 0.01$), the K-S test statistic and critical values are 0.105 and 0.144 respectively. The probability value is also greater than α that is 0.452. Based on these results, we clearly failed to reject the null hypothesis. We randomly collected 12 data points each of subgroup size $n = 6$ and these samples reasonably satisfy the inverse *Maxwell* assumption.

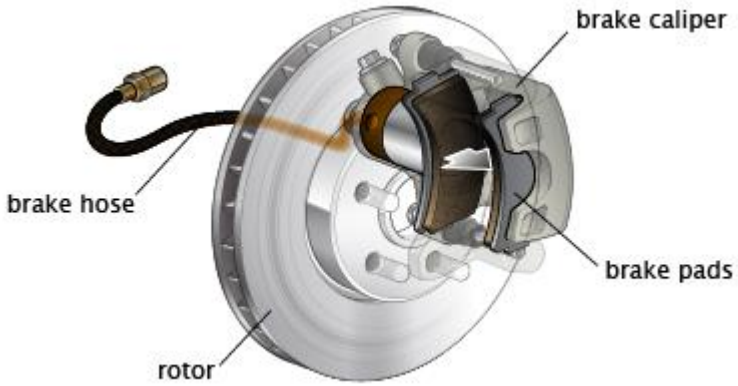

Figure 6.3: Vehicle breaking components [68].

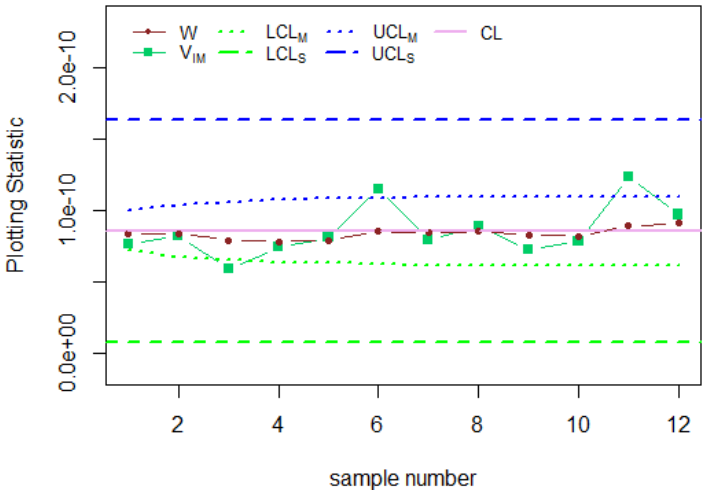

Figure 6.4: Combined IM-VEWMA control chart at δ=1.

Now for the construction of CIM-VEWMA control chart, based on the real data used in this example and Section 3, all the required numerical values of plotting statistics and control limits are calculated and provided into Table 6.6. Here, the estimated value of the MLE is $\bar{V}_{IM} =$

8.577×10^{-11} and this will consider as the center line. We also consider the in-control ARL is 370 and $\lambda = 0.18$. To monitor this process whether it is in statistical control or not we construct the proposed CIM-VEWMA chart in Figure 6.4. In Section 6.3, we observe that the proposed chart is more sensitive to shifts than the individual V_{IM} and $IMEWMA$ charts and to examine this effectiveness on the real-life scenario in Figures 6.5 and 8, we consider 25% and 50% increment of shifts respectively after the 7th data points. Based on Figures 6.4-6.6, we made the following observations:

Table 6.6: Plotting statistics and Control limits of CIM-VEWMA chart for cars' brake pads data.

$CIM - VEWMA$ chart						
	V_{IM} chart			$IMEWMA$ chart		
Sample number	V_{IM}	LCL_S	UCL_S	z	LCL_M	UCL_M
1	7.656	0.806	16.347	8.410	7.177	9.975
2	8.218			8.376	6.767	10.385
3	5.931			7.936	6.537	10.615
4	7.427			7.844	6.396	10.756
5	8.115			7.893	6.307	10.846
6	11.479			8.538	6.248	10.904
7	7.973			8.437	6.210	10.943
8	8.934			8.526	6.184	10.968
9	7.252			8.297	6.167	10.985
10	7.807			8.209	6.156	10.996
11	12.390			8.961	6.148	11.004
12	9.729			9.100	6.143	11.009

Note: Units are 1.00×10^{-11} km.

1. Figure 6.4 visualizes that the process is in-control because none of the out of control criteria including a point outside the control limits, a run of seven points or more, a run of points beyond some secondary limits, the points are too close to the central line, presence of trends and presence of cycles provided in [71] present in it.
2. From the plotted Combined IM-VEWMA chart in Figure 6.5, we observe that the 11th and 12th samples are out of IMEWMA control limits whereas the V_{IM} chart doesn't give any signal because of the insensitivity of the V_{IM} chart to small shifts. To surpass

this confusion, based on our proposed chart we can easily conclude that the process is out-of-control and detect 2 signals where the shift is 25% increased.

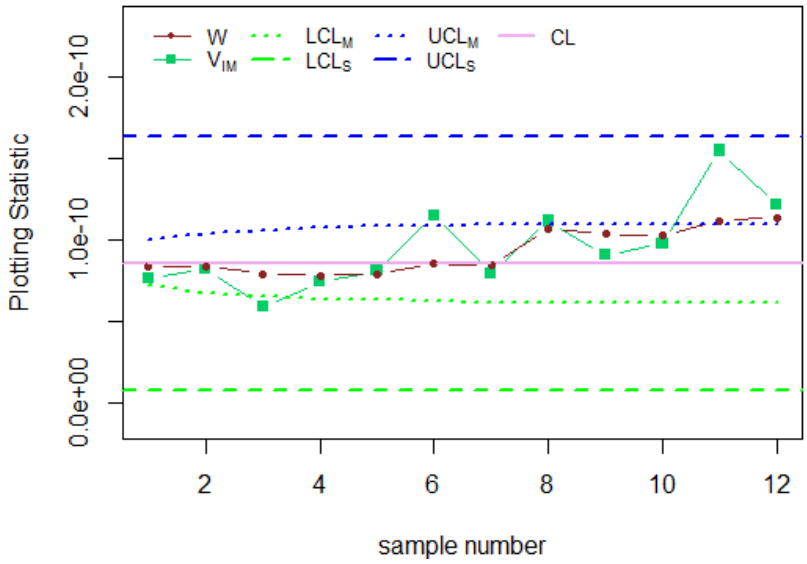

Figure 6.5: Combined IM-VEWMA control chart at δ=1.25.

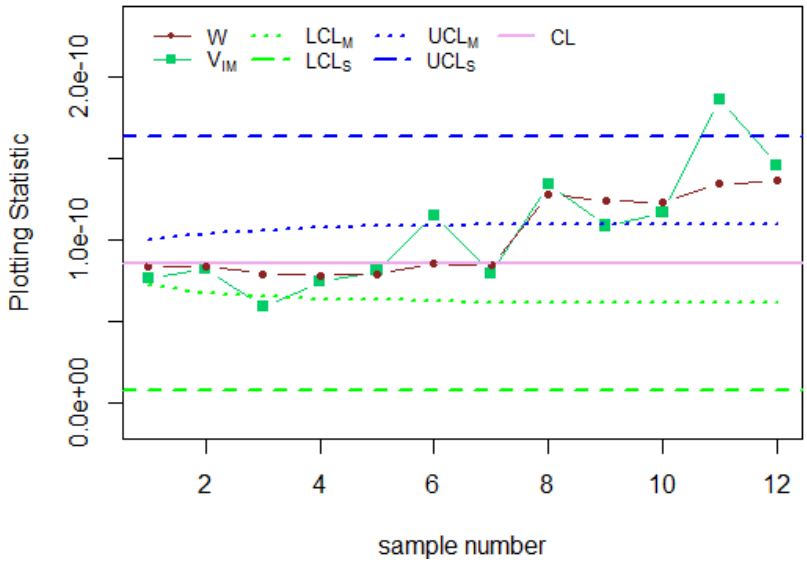

Figure 6.6: Combined IM-VEWMA control chart at δ=1.50.

3. The combined IM-VEWMA chart also provides a precise out-of-control signal when $\delta = 1.5$. The proposed chart gives 6 signals where all the increased shifts are detected by IMEWMA and V_{IM} catches one signal that is the 11^{th} sample (see Figure 6.6). Clearly, our proposed CIM-VEWMA chart provides an edge over the other charts which is in conformity with our findings in Section 6.3.

6.5 Summary of the CIM-VEWMA control chart

One of the major goals of control chart is to detect shifts as quick as possible whether the shifts are large or small. In this article, to accomplish this purpose, a new control chart by consolidating the characteristics of V_{IM} and IMEWMA charts, called CIM-VEWMA control chart has proposed for an inverse *Maxwell* process. The study evaluated the RL performance of the suggested chart and showed that the RL distribution of the CIM-VEWMA chart is positively skewed. The sensitivity of this new control chart to small, moderate and large shifts is exposed through several RL properties including MRL and RARL. The proposed chart has become more sensitive to detect shifts as the small smoothing constant value decrease. The comparative analysis has revealed that the proposed chart has significant deal of improvements for detecting both transient and persistent variations compared with lone V_{IM}, IMEWMA and IMCUSUM control chart as well. An application example based on the lifetime of car brake pads has also demonstrated the superiority of the proposed chart with the existing counterparts.

CHAPTER SEVEN

CONCLUSIONS AND RECOMMENDATIONS

In this thesis we introduce the inverse *Maxwell* distribution along with its several distributional and reliability characteristics including MGF, CF, mode and moments. We have also discussed the estimation procedure of the only scale parameter of the inverse *Maxwell* distribution under maximum likelihood estimation. Here, we develop two memory type control charts namely IMEWMA and IMCUSUM and a combined control chart named as CIM-VEWMA to diagnose the inverse *Maxwell* production process more effectively and efficiently as quick as possible. We measure the performance of the newly proposed control chart under several run length properties and some overall performance identifying tools. The both developed control charts are sensitive to small and moderate assignable cause variations of scale parameter σ in process monitoring. The comparison of the existing charts with our suggested charts is also constructed add we observe that the both proposed charts are performing better than the only exiting Shewhart type control chart under inverse *Maxwell* distribution named as V_{IM} control chart. The comparison study also reveals that the CIM-VEWMA control chat outperform than the IMEWMA control chart especially for moderate and large shifts. Finally, simulation study and real-life example have been demonstrated.

In the literature only Shewhart type control chart is available for an inverse *Maxwell* production process whereas to monitor normal production process various memory type of control chart is available. In the current thesis, we develop two memory type control charts under inverse *Maxwell* distribution and evaluate their performance.

In Chapter three, we introduced different properties of inverse *Maxwell* distribution. The MGF and CF of the inverse *Maxwell* distribution are derived. The moments of the inverse *Maxwell* distribution have been studied as well. To verify the applicability of this distribution in survival analysis, the survival and hazard curve is also presented.

In Chapter four, we propose a memory type control chart for an inverse Maxwell process namely IMCUSUM control chart. The performance of the developed chart is provided through average run length, standard deviation of run length and performance comparison index along with its construction procedures. The comparative analysis suggest that it is superior to the existing Shewhart type control chart for small shifts. Finally, a simulation study describe the

development simplicity and the necessity of this proposed chart is confirmed with a real-life application.

In Chapter five, the design structure of the IMEWMA control chart is provided. It is a memory type control chart under IMD that accumulates all information in the entire sequence of sample observations to identify persistent cause variations. The run length study suggests that the RL distribution is positively skewed for IMEWMA chart. We also compare the IMEWMA control chart with V_{IM} control chart and observe that the ARL and MRL values of the new chart is less than the V_{IM} chart. It suggests that the IMEWMA control chart is better for detecting assignable cause variations in IMD production process. A simulation study is also conducted here to visualize the simple design procedure. Finally, an application over the cars brake pads lifetime is discussed.

In Chapter six, the Combined IM-VEWMA chart is proposed which is also the member of memory type control chart. This chart contains not only the information about the process acquired from the last sample observation but also accumulate all information in the entire sequence of sample observations to identify persistent cause variations. It means that it uses both past and present information at the same time. Like as IMEEWMA, this charts' RL distribution is also positively skewed. So, we use EQL, RARL and PCI for evaluating its variations detecting ability along with ARL and MRL. A comparison study based on the following tools revels that the proposed CIM-VEWMA chart is capable to identify both transient and persistent cause variations faster than the existing V_{IM} control chart and newly developed IMEWWMA control chart. Though a lack of performance is observed than IMCUSUM chart for small variations. An example based on the lifetime of car brake pads has also demonstrated the superiority of the proposed chart with the existing counterparts.

7.1 Recommendations

In this section we would like to recommend the use of inverse *Maxwell* distribution and also provide some other types of control chart those can be developed under IMD for further future research. Some recommendations are given underneath.

1. We studied the only scale parameter to monitor the IMD production process under IMCUSUM, IMEWMA and CIM-VEWMA control chart. We haven't considered the mean of the inverse *Maxwell* distribution to monitor its production process.
2. We combine the Shewhart type control chart with EWMA control chart under IMD while several other combinations can also be made such as Shewhart with CUSUM and EWMA with CUSUM.

3. Several run length schemas can be used to increase the effectiveness of the control charts under IMD.
4. The scope of this study may be extended to multivariate structure.

References

[1] J. S. Oakland, Statistical Process Control, 5th ed., Burlington:: Butterworth-Heinemann, 2003.

[2] R. J. M. M. Does, K. C. B. Roes and A. Trip, Statistical Process Control in Industry, Netherlands: Kluwer; Dordrecht, 1999.

[3] D. M. Hawkins and D. H. Olwell, Cumulative Sum Charts and Charting for Quality Improvement, New York: Springer, 1998.

[4] D. C. Montgomery, Introduction to Statistical Quality Control, 6th ed., New York: Wiley, 2009.

[5] M. Aslam, N. Khan and M. Azam, "X-Bar Control Charts for Non-Normal Correlated Data Under Repetitive Sampling," *Journal of Testing and Evaluation,* vol. 44, no. 4, pp. 1756-1767, 2016.

[6] M.-Y. Liao and H.-C. Ling, "Effective Control Chart for Monitoring the Capability Stability of Non-Normal Processes Having S-Type Quality," *Journal of Testing and Evaluation,* vol. 46, no. 3, pp. 1196-1208, 2018.

[7] P. S. Rao and C. Ratnam, "Vibration Based Damage Identification Using Burg's Algorithm and Shewhart Control Charts," *Journal of ASTM International,* vol. 8, no. 4, pp. 1-12, 2011.

[8] W. H. Woodall, "Controversies and Contradictions in Statistical Process Control," *Journal of Quality Technology,* vol. 32, no. 4, pp. 341-350, 2000.

[9] S. Roberts, "Control chart tests based on geometric moving averages," *Technometrics,* vol. 1, pp. 239-250, 1959.

[10] E. S. Page, "Continuous inspection schemes," *Biometrika,* vol. 41, pp. 100-115, 1954.

[11] Bhattacharya, Tyagi, R. K. and S. K., "Bayes estimation of the Maxwell's velocity distribution function," *Statistica,* vol. 29, no. 4, p. 563–567, 1989.

[12] Bhattacharya, Tyagi, R. K. and S. K., "A note on the MVU estimation of the Maxwell's failure distribution," *Estadistica,* vol. 41, p. 73–79, 1989.

[13] P¨oschel, N. V. Brilliantov and Thorsten, "Deviation from Maxwell Distribution in Granular Gases with Constant Restitution Coefficient," 27jun,1999.

[14] Garrison and Zhigilei, "Velocity distributions of molecules ejected in laser ablation," *Applied Physics Lette,* vol. 71, no. 4, pp. 551-553, 1997.

[15] ""What is LIBS? - Applied Spectra," Applied Spectra, 2016. [Online]. Available:http://appliedspectra.com/technology/libs.html. [Accessed 23 august,2017]".

[16] ""How do Airbags Work?," Buzzle, 2016. [Online]. Available:http://www.buzzle.com/articles/how-do-airbags-work.html. [Accessed 23 August,2017]".

[17] S. Sato and J. Inoue, "Inverse gaussian distribution and its application," *Electronics and communications in japan (part iii: Fundamental Electronic Science),* vol. 77, no. 1, pp. 32-42, 1994.

[18] N. Keyfitz, Applied mathematical demography, 2nd ed., New York: Springer, 1985.

[19] N. Keyfitz, "Decomposition and reassembly of the age-time distribution," *Research paper series,* vol. 49.

[20] Harrington and L. Maxim, "On optimal two stage cluster sampling for aerial surveys with detections errors," *Photogrammetric engineering and remote sensing,* vol. 50, no. 11, pp. 1613-1627, November,1984.

[21] chhikara and Raj, The inverse Gaussain distributin:Theory, Methodology and Applications.

[22] S. Y. Arafat, M. Hossain, M. Omar and M. Riaz, "On the Development of Inverse Maxwell Distribution with Industrial Application".

[23] R.S.Srivastava and K. L. S. a. R.S., "Inverse Maxwell Distribution as a Survival Model, Genesis and Parameter Estimation," *Research Journal of Mathematical and Statistical Sciences,* vol. 2, no. 7, pp. 23-28, 2014.

[24] R.S.Srivastava and K. L. Singh, "Estimation of the Parameter in the Size-Biased Inverse Maxwell Distribution," *International Journal of Statistika and Mathematika,* vol. 10, no. 3, pp. 52-55, 2014.

[25] R.S.Srivastava and S. K. Lata, "Bayesian Estimation of Parameter of Inverse Maxwell Distribution via Size-Biased Sampling," *International Journal of Science and Research (IJSR),* vol. 3, no. 9, pp. 1835-1839, 2014.

[26] M. P. Hossain, M. H. Omar and M. Riaz, "New V control chart for the Maxwell distribution," *Journal of Statistical Computation and Simulation,* vol. 87, no. 3, pp. 594-606, 2017.

[27] M. Hossain, M. Omar and M. Riaz, "Estimation of mixture Maxwell parameters and its possible industrial application," *Computers & Industrial Engineering,* vol. 107, pp. 264-275, 2017.

[28] C. A. Acosta-Mejia, J. J. Pignatiello and B. V. Rao, "A comparison of control charting procedures for monitoring process dispersion," *IIE Transactions,* vol. 31, no. 6, p. 569–579, 1999.

[29] R. A. Sanusi, N. Abbas and M. Riaz, "On efficient CUSUM-type location control charts using auxiliary information," *Quality Technology & Quantitative Management,* vol. 15, no. 1, pp. 87-105, 2018.

[30] Z. Wu, J. Jiao, M. Yang, Y. Liu and Z. Wang, "An enhanced adaptive CUSUM control chart," *IEE Transactions,* vol. 41, no. 7, pp. 642-653, 2009.

[31] L. Shu and W. Jiang, "A Markov Chain Model for the Adaptive CUSUM Control Chart," *Journal of Quality Technology,* vol. 38, no. 2, pp. 135-147, 2006.

[32] P. Castagliola and P. E. Maravelakis, "A CUSUM control chart for monitoring the variance when parameters are estimated," *Journal of Statistical Planning and Inference,* vol. 141, no. 4, pp. 1463-1478, 2011.

[33] F. F. Gan, "Design of Optimal Exponential CUSUM Control Charts," *Journal of Quality Technology ,* vol. 26, no. 2, pp. 109-124, 1994.

[34] F. F. Gan, "An optimal design of CUSUM control charts for binomial counts," *Journal of Applied Statistics,* vol. 20, no. 4, pp. 445-460, 2006.

[35] J. R. Jiao and P. T. Helo, "Optimization design of a CUSUM control chart based on taguchi's loss function," *The International Journal of Advanced Manufacturing Technology,* vol. 35, no. 11-12, p. 1234–1243, 2008.

[36] S. Chowdhury, A. Mukherjee and S. Chakraborti, "Distribution-free Phase II CUSUM Control Chart for Joint Monitoring of Location and Scale," *Quality and Reliability Engineering International ,* vol. 31, no. 1, 2014.

[37] M. C. Testik, "Conditional and marginal performance of the Poisson CUSUM control chart with parameter estimation," *International Journal of Production Research,* vol. 45, no. 23, pp. 5621-5638, 2007.

[38] M. P. Hossain, R. A. Sanusi, M. H. Omar and M. Riaz, "On designing Maxwell CUSUM control chart: an efficient way to monitor failure rates in boring processes," *The International Journal of Advanced Manufacturing Technology,* vol. 100, no. 5-8, p. 1923–1930, 2019.

[39] S. W. Roberts, "Control chart tests based on geometric moving averages," *Technometrics,* vol. 1, pp. 239-250, 1959.

[40] C. M. Borror, C. W. Champ and S. E. Rigdon, "Poisson EWMA Control Charts," *Journal of Quality Technology,* vol. 30, no. 4, pp. 352-361, 1998.

[41] F. F. Gan, "Monitoring Poisson Observations Using Modified Exponentially Weighted Moving Average Control Charts," *Communications in Statistics - Simulation and Computation,* vol. 19, no. 1, pp. 103-124, 2007.

[42] F. F. Gan, "Monitoring observations generated from a binomial distribution using modified exponentially weighted moving average control chart," *Journal of Statistical Computation and Simulation,* vol. 37, no. 2, pp. 45-60, 2007.

[43] S. T. A. Niaki and P. Jahani, "The economic design of multivariate binomial EWMA VSSI control charts," *Journal of Applied Statistics,* vol. 40, no. 6, pp. 1301-1318, 2013.

[44] Fong-JungYu, Yung-YuYang, Ming-JaanWang and ZhangWu, "Using EWMA control schemes for monitoring wafer quality in negative binomial process," *Microelectronics Reliability,* vol. 51, no. 2, pp. 400-405, 2011.

[45] C. M. Borror, D. C. Montgomery and G. C. Runger, "Robustness of the EWMA Control Chart to Non-Normality," *Journal of Quality Technology,* vol. 31, no. 3, pp. 309-316, 1999.

[46] S. A. Abbasi, M. Riaz, A. Miller, S. Ahmad and H. Z. Nazir, "EWMA Dispersion Control Charts for Normal and Non-normal Processes," *Quality and Reliability Engineering International,* vol. 32, no. 6, pp. 204-218, 2014.

[47] P. E. Maravelakis, J. Panaretos and S. Psarakis, "An Examination of the Robustness to Non Normality of the EWMA Control Charts for the Dispersion," *Communications in Statistics - Simulation and Computation,* vol. 34, no. 4, pp. 1069-1079, 2005.

[48] M. C. Testik, G. C. Runger and C. M. Borror, "Robustness properties of multivariate EWMA control charts," *Quality and Reliability Engineering International,* vol. 19, no. 1, pp. 786-796, 2002.

[49] S. M. M. Raza, M. Riaz and S. Ali, "EWMA Control Chart for Poisson–Exponential Lifetime Distribution Under Type I Censoring," *Quality and Reliability Engineering International,* no. 32, pp. 955-1005, 2016.

[50] L. ZHANG, "EWMA Charts for Monitoring the Mean of Censored Weibull Lifetimes," *Journal of Quality Technology,* vol. 36, no. 3, pp. 321-328, 2004.

[51] O. H. Arif, M. Aslam and C. H. Jun, "EWMA np Control Chart for the Weibull Distribution," *Journal of Testing and Evaluation,* vol. 45, no. 3, pp. 1022-1028, 2017.

[52] W. L. Teoh, J. Lim, Z. L. Chong and W.C.Yeong, "Optimal Designs of EWMA Charts for Monitoring the Coefficient of Variation Based on Median Run Length and Expected Median Run Length," *Journal of Testing and Evaluation,* vol. 47, no. 1, 2019.

[53] J. M. Lucas and M. S. Saccucci, "Exponentially Weighted Moving Average Control Schemes: Properties and Enhancements," *TECHNOMETRICS,* vol. 32, no. 1, pp. 1-12, 1990.

[54] J. O. Westgard, T. Groth, T. Aronsson and C. H. d. Verdier, " Combined Shewhart-CUSUM Control Chart for Improved Quality Control In Clinical Chemistry," *Clinical Chemistry ,* vol. 23, no. 10, pp. 1881-1887, 1977.

[55] W. H. Woodall and M. A. Mahmoud, "The Inertial Properties of Quality Control Charts," *Technometrics,* vol. 47, no. 4, pp. 425-436, 2005.

[56] M. Klein, "Composite Shewhart-EWMA statistical control schemes," *IIE Transactions,* vol. 28, no. 6, pp. 475-481, 1996.

[57] G. O. Tolley and J. R. English, "Economic designs of constrained EWMA and combined EWMA-$\bar{X}$ control schemes," *IIE Transactions,* no. 33, pp. 429-436, 2001.

[58] B. F. Simoes, E. K. Epprecht and A. F. Costa, " Performance Comparisons of EWMA Control Chart Schemes," *Quality Technology and Quantitative Management,* vol. 7, no. 3, pp. 249-261, 2010.

[59] L. Zhang, M. Bebbington, K. Govindaraju and C. Lai, " Composite EWMA control charts," *Communications in Statistics-Simulation and Computation,* vol. 33, no. 4, pp. 1133-1158, 2004.

[60] N. Abbas, M. Riaz and R. J. M. Does, " Mixed exponentially weighted moving average–cumulative sum charts for process monitoring," *Quality and Reliability Engineeering International,* vol. 29, no. 3, pp. 345-356, 2012.

[61] G. Capizzi and G. Masarotto, " Combined Shewhart-EWMA control charts with estimated parameters," *Journal of Statistical Computation and Simulation,* vol. 80, no. 7, pp. 793-807, 2010.

[62] M. C. Morais and A. Pacheco, "Combined CUSUM–Shewhart Schemes for Binomial Data," *Economic Quality Control,* vol. 21, no. 1, pp. 43-57, 2006.

[63] V. Abel, "On one-sided combined Shewhart-CUSUM quality control schemes for Poisson counts," *Computational Statistics Quaterly,* no. 6, pp. 31-39, 1990.

[64] E. Henning, A. C. Konrath, C. d. C. Alves, O. M. F. C. Walter and R. W. Samohyl, "Performance Of A Combined Shewhart-Cusum Control Chart With Binomial Data For Large Shifts In The Process Mean," *Int. Journal of Engineering Research and Application,* vol. 5, no. 8, pp. 235-243, 2015.

[65] E. Page, "Continuous inspection schemes," *Biometrika,* vol. 41, no. 1/2, pp. 100-114, 1954.

[66] S. V. Crowder, "A Simple Method for Studying Run-Length Distributons of Exponentially Weighted Moving Average Charts," *Technometrics,* vol. 29, no. 4, pp. 401-407, 1987.

[67] Z. Wu, M. Yang, W. Jiang and M. B.C.Khoo, "Optimization designs of the combined Shewhart-CUSUM control charts," *Computational Statistics & Data analysis,* vol. 53, no. 2, pp. 496-506, 2008.

[68] Y. Ou, Z. Wu and F. Tsung, " A comparison study of effectiveness and robustness of control charts for monitoring process mean," *International Journal of Production Economics,* vol. 135, no. 1, pp. 479-490, 2012.

[69] J. F. Lawless, Statistical Models and Methods for Lifetime Data, 2nd ed., Wiley-Interscience, 2000, p. 69.

[70] Q.-U.-A. Khaliq, M. Riaz and S. Ahmad, "On designing a new Tukey-EWMA control chart for process monitoring," *The International Journal of Advanced Manufacturing Technology,* vol. 82, no. 1-4, p. 1–23, 2016.

[71] "“R: What is R?” [Online],". Available: https://web.archive.org/web/20190130112835/https://www.r-project.org/about.html.. [Accessed 02 January 2019].

[72] S. A. Klugman, H. H. Panjer and G. E. Willmot, Loss Models From Data To Decisions, 4th ed., WILEY, 2012.

[73] S. Gupta and V. Kapoor, Fundamentals of Applied Statistics, New Delhi: Sultan chand and Sons, 2006.

[74] P. Balu, "Compositions, Functions, and Testing of Friction Brake Materials and Their Additives".

[75] K. H. Singh, A. Kumar and R. Kumar, "Optimization of Quality and Performance of Brake Pads Using Taguchi’s Approach," *International Journal of Scientific & Engineering Research,* vol. 5, no. 7, pp. 632-639, 2014.